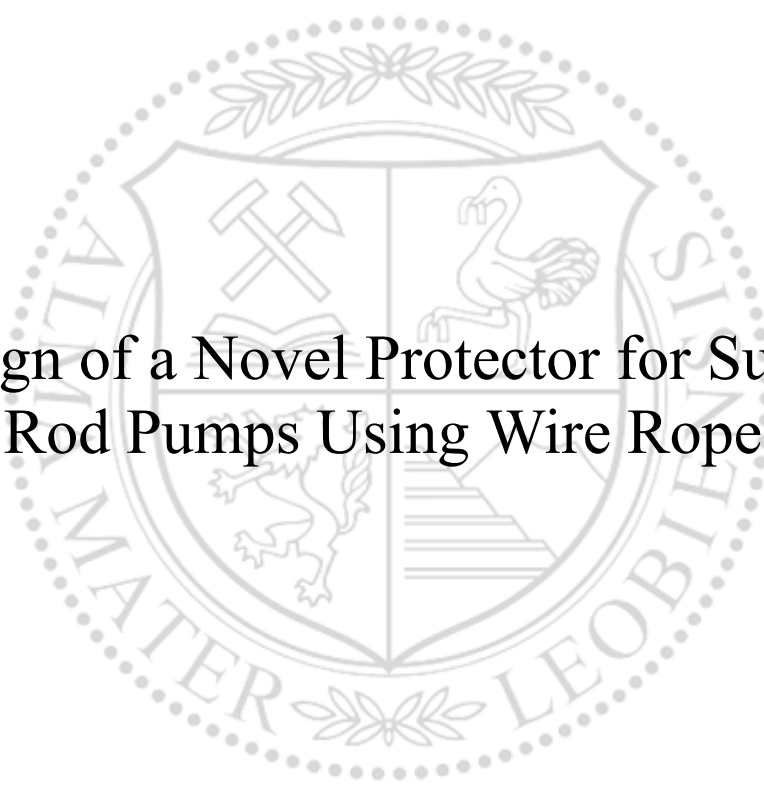MONTAN
UNIVERSITÄT
LEOBEN

Chair of Petroleum and Geothermal Energy Recovery

Master's Thesis

Design of a Novel Protector for Sucker Rod Pumps Using Wire Rope

Ramzy Albishini

September 2019

AFFIDAVIT

I declare on oath that I wrote this thesis independently, did not use other than the specified sources and aids, and did not otherwise use any unauthorized aids.

I declare that I have read, understood, and complied with the guidelines of the senate of the Montanuniversität Leoben for "Good Scientific Practice".

Furthermore, I declare that the electronic and printed version of the submitted thesis are identical, both, formally and with regard to content.

Date 18.09.2019

_____

Signature Author
Ramzy, Albishini
Matriculation Number: 01629934

Zusammenfassung

Die Erfindung der Stangenführung oder des Stangen-Protektors, unabhängig davon ob hin- und hergehend oder rotierend verwendet, dient nicht nur zur Ausrichtung des Pumpgestänges in der Mitte des Bohrloches, sondern auch als Paraffinschaber.

Seit 1927 hat sich das Material und die Konstruktion stark verändert, um sowohl das Pumpgestänge selbst als auch die Rohre besser zu schützen und damit die mittlere Ausfallszeit (MTBF) zu erhöhen.

Der Zweck dieser Studie ist es, ein neues Design für Protektoren zu entwickeln, das speziell für Drahtseile verwendet wird, die Gestängetiefpumpen aktivieren.

Da die Drehvorrichtung des konventionellen Pumpgestänges nicht für Drahtseilen eingesetzt werden kann, wurde der Schutz mit vier Rippen ausgeführt, die einen Schabeeffekt mit 360° an der Innenwand des Rohres bilden. Dieser Schutz besteht aus zwei identischen Teilen, die auf

CFD-Simulationen wurden mit der Software ANSYS durchgeführt, um die richtige Länge und den richtigen Durchmesser des entworfenen Protektors zu definieren, was zu akzeptablen Druckverlusten und erodierbaren Verschleißvolumen führte.

Schlagwörter: Gestängetiefpumpe, Artificial Lift Systems, Drahtseile, Stangen-Protektor, Erodierbares Volumen

Abstract

The invention of the rod guide or protector, whether used in reciprocating or rotating sucker rod strings, is meant not only to centralize the rod strings but also to serve as a paraffin scrapper.

Since 1927, rod guides have changed considerably in terms of the materials used and design, in order to provide more protection for rod strings as well as tubing, hence, increasing the mean time between failures (MTBF).

The purpose of this study is to provide a design for protectors, used specifically for wire ropes which activate downhole pumps.

Since the rod rotator cannot be utilized in a sucker rod pump using wire ropes, the protector was designed with four ribs forming circumferential scraping effect with 360° on the interior wall of the tubing. This protector consists of two identical parts that can be installed on the wire rope in the field.

CFD simulations were performed with the software Ansys to define the proper length and diameter of the designed protector, which led to acceptable pressure drops and erodible wear volume.

Keywords: sucker rod pumping; artificial lift systems; wire rope; rod guide; EWV; CFD.

Abbreviations

SRP	Sucker Rod Pump
EWV	Erodible Wear Volume
PEEK	Polyether Ether Ketone
PAEK	Polyaryletherketone
PPA	Polyphthalamide
PPS	Polyphenylene sulphide
PEUHMW	Ultra-high-molecular-weight polyethylene
MTBF	Mean Time Between Failure
SST-kw	The Shear-Stress Transport (SST) k-w Model
API	American Petroleum Institute
PCP	Progressing cavity pump
NORSOK	Norwegian petroleum industry Standard
DIN ISO 286	German Institute of Standardization and International Organization for Standardization

Table of Content

1 Introduction

Sucker rod pump is considered to be one the most popular artificial lift system used in oil and gas industry for many reasons such as the cost, efficiency, ease of operation and control. Due to those considerations, continuous improvement of the sucker rod pumping system has being pursued.

One of these improvements is the replacement of the rod string by a wire rope. This new system brings a lot of advantages like reduction of the maximum load on the polished rod and accordingly saving power. Other benefits include eliminating the coupling failure and allowing the operation of the pump in deviated wells.

The purpose of this work is to design protectors for wire rope activated pump. For simplification, the term "protector" will be used interchangeably with "rod guide".

The first and the second chapters go through the functions of rod guides and the methods of spacing them onto the rod strings.

The aim of the third chapter is to offer an appropriate approach for rod guide classifications, that can cover the various designs manufactured by different companies or the ones available in literature, while the fourth chapter analyses the factors, which can affect the rod guide efficiency in terms of material and design.

The description of this protector which was designed in Solidworks is explained in the fifth chapter, while the flow simulation using ANSYS is disclosed in chapter 6.

Finally, the results and conclusion are detailed in the seventh chapter with further recommendations in chapter 8.

2 Fundamentals

This chapter discusses the basic principles of rod guides and their use in rod pumping. In addition, it goes through the criteria to be considered for Rod Guides installation.

2.1 Rod pumping

Rod pumping is one of the artificial lift methods that involves the use of a downhole pump to increase the lifting head and overcome the sum of flowing pressure losses that occur from the bottom of the well to the surface.

In sucker rod pumps, the downhole pump is a positive displacement pump which is activated by a rod string that provides the link from the surface unit to the pump. The rod string reciprocates in order to actuate pump plunger and produce the fluid in sucker rod pump (2). However, in progressive cavity pumps, the rod strings rotates in order to activate the downwole pump which consists of two parts: the stator made of helical steel with elastomer sleeves, and the rotator made of helical steel that matches the stator configuation (1). Figure 1 provides the main components for a sucker rod pump, and Figure 2 is for a progressive cavity pump.
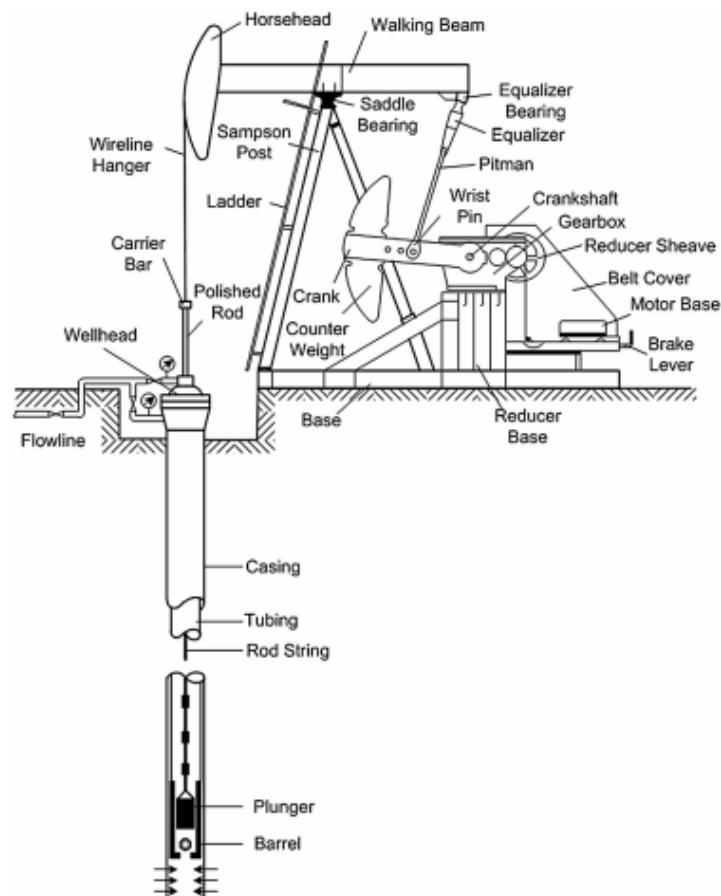
Figure 1 main components of SRP (2)
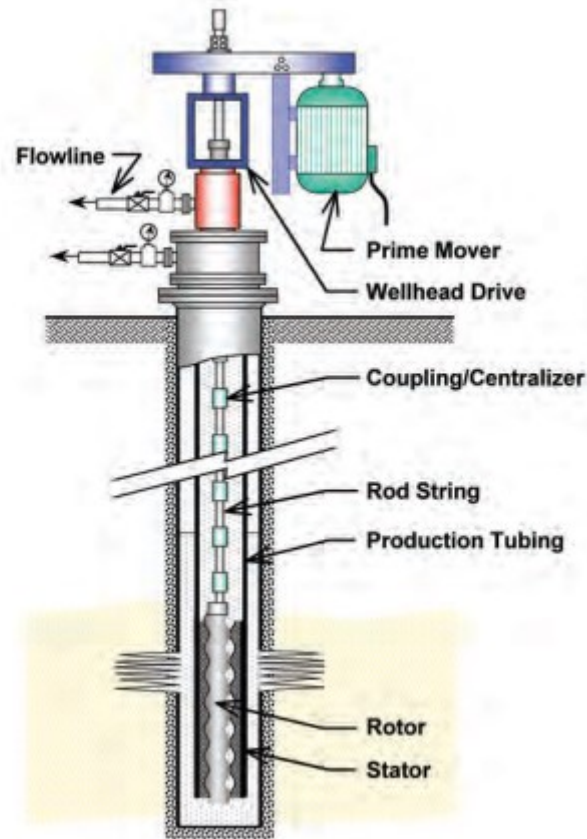
Figure 2 typical PCP (1)

2.2 Functions of a Rod Guide

The functions of rod guides can be summarised as the following:

1) Centralising the rod string, which consists of many rods, each connected to another by couplings.

    Due to many reasons like well deviation, flexing of the sucker rods caused by the reciprocating movement of sucker rod, or tubing buckling, the rod string will come into contact with the tubing inevitably.

    Without rode guides the rod string will rub against the interior wall of the tubing causing wear in the rod string and mainly in the couplings, as they have the largest diameter in the rod string. Additionally, they will create holes in the tubing which results in expensive repair operations and non-productive time. Rod guides are typically installed on sucker rods. By having a diameter bigger than the couplings, they can prevent undesirable metal to metal contact between reciprocating or rotating rods and the tubing.

2) Placement of the rod guides in specific locations stabilises the pump and prevents valve rod from breaking or bending (1).

3) Removing the precipitants from the interior wall of production tubing and reducing the number of costly oil and chemical treatments.

These precipitants occur as the well fluid rises to the surface, where the temperature is reduced and insufficient to retain paraffin in the liquid state, paraffin congeals and accumulates in the tubing, causing the production tubing to clog and decrease the production.

2.3 Rod Guides spacing

Rod guide design (spacing, geometry, material selection) should be integrated with the wellbore survey, dynamometer card, well-operating conditions, and rod pumping design to obtain the optimum performance (3).

Rod guide spacing defines the number of rod guides per rod, and the way it is arranged along the sucker rod string. Spacing will play a vital role in rod pumping design especially in deviated wells (4).

As standard practice, rod guides should be placed on or between the pump-handling pony rod, the sinker bars and the first two sucker rods above the sinker bar (1).

Regarding paraffin scraping function, there is a rule of thumb formula which defines the number of rod guides per sucker rod. This is equal to sucker rod length (inches) divided by stroke length (inches) plus 1.

For centralising the rod string and avoiding rod /tubing wear there are two approaches:

1) **Trial and error method**: applying rod guide design from other wells with similar conditions of fluid production, specific gravities, water cut, well depth, stroke length, pump size, etc.

   If the rod guide wear is more significant than anticipated more rod guides are added.

   The problem with this method is that it might lead to recommending more rod guides than necessary which can trigger several problems like power requirement, erosion and corrosion problems.

2) **Based on rod buckling**: this method uses Euler's equation which can calculate the compressive stress required to buckle the sucker rod and put the rod, or the couplings in contact with tubing wall.

   The static test have shown that by placing the rod guides 16 inches away from the sucker rod ends in asymmetrical configuration, as shown in Figure 3. The sucker rod can tolerate higher compressive stresses than setting the rod guides symmetrically.
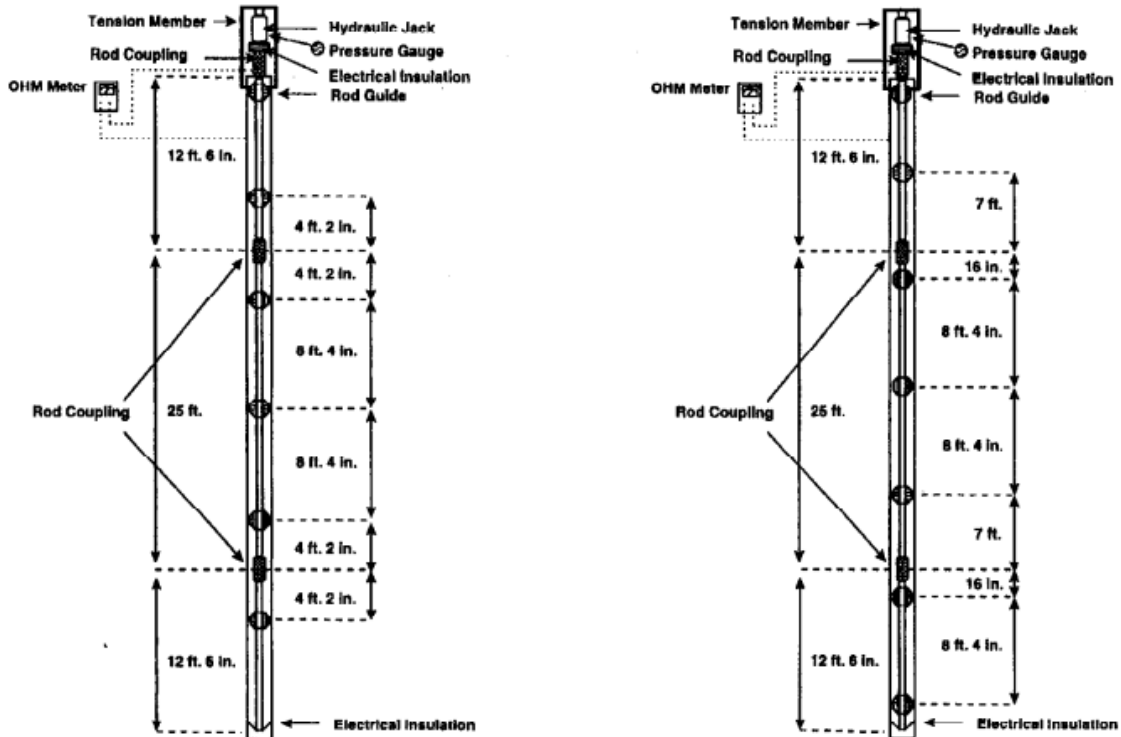
Figure 3 on the left side three rod guides are symmetrically installed, on the right side three rod guides are installed in asymmetrical configuration (5).

It is also recommended to use the Lubinski curve when the tubing anchor is set several hundred feet above the seating nipple or if it is not run at all.

Using the formula to calculate the buckling distance and the Lubinski curve (Figure 4), the number of rod guides per rod can be determined.

The formula is to determine the distance that unanchored tubing will buckle above the seating nipple. For tubing $2^7/_8$ inches OD API tubing, Buckling distance $= \dfrac{Fo}{5,7}$ ft. Where Fo is the fluid load on the gross plunger area.
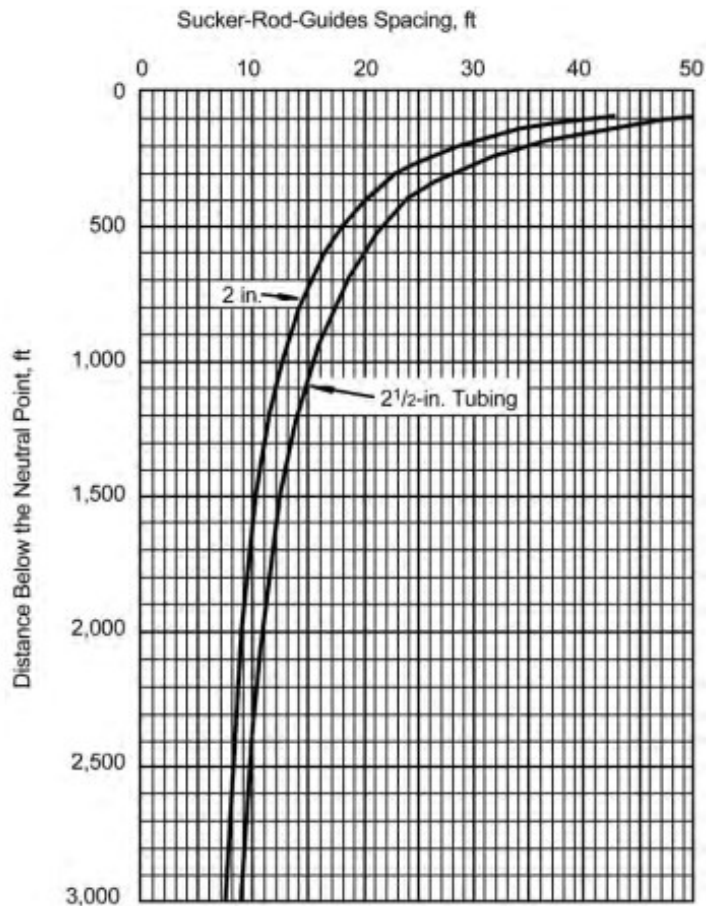
Figure 4 Minimum recommended number of rod guides that prevent buckling for normal sucker rod production tubing. (1)

Some companies provide computer applications to provide the optimum rod guides placement, like SROD developed by Lufkin Automation for vertical and deviated wells. This application is based on rod buckling considerations with surface unit and wave equation solution, rod and guide properties to calculate the maximum side load on each rod in order to determine the number of rod guides. (4)

3 Rod Guide Types

The early design of rod guides was intended for them to act as paraffin scrapper. This was a piece of metal welded on sucker rods. That triggered significant wear in the tubing string and led to the invention of moulded plastic guides on sucker rods.

The need to reduce turbulence and hydraulic drag forces paved the way for manufacturing extended tapered rod guides and different designs with different vane shapes. Later on, the wide vane design came into use with a large bearing surface. Lately, the rotating rod guides have been introduced and used in PCPs.

This chapter attempts to cover several rod guide designs found in the literature review. Different products from different companies will also be presented in this chapter.

3.1 Characterisation based on installation methods

Rod guide is installed on the sucker rod, either being moulded in the factory on the sucker rod or fixed at the well site.

3.1.1 Moulded rod guides

This type of rod guide is the most common. They are manufactured by injection moulding process. Their design provides a ridged lock on the rod against the axial load, where the body and the vanes are moulded simultaneously. Such a design is preferably used in harsh well conditions, but it is more expensive than field installed rod guides. (6)

3.1.2 Field installed rod guides

These guides maintain their grip on the rod by friction forces and must tolerate high axial loads without slipping. Some of these guides require an encapsulated metal insert to achieve locking strength. Although they prove to be cost-effective as a result of shortening the downtime, their grip on strength makes them be preferably used in low volume and low-temperature wells. The material of the rod guide plays an important role in the lock-on strength. (7)

The following presents different designs of field installed guides:

1) **Twisted on design**: it consists of a central longitudinal channel which is slightly in a smaller diameter than rod diameter so that the rod guide can be held and mounted on the rod against the axial forces resulted from reciprocating movement. It has two mounting slots in opposite directions. When the rod guide rotates around the rod in a clockwise direction, the mounting slots will receive the rod. This guide has an intermediate reduced thickness portion to facilitate the installations of rod guide by permitting flexure of opposite end portions. Figure 5 shows a twisted-on rod guide designed by NORRIS.
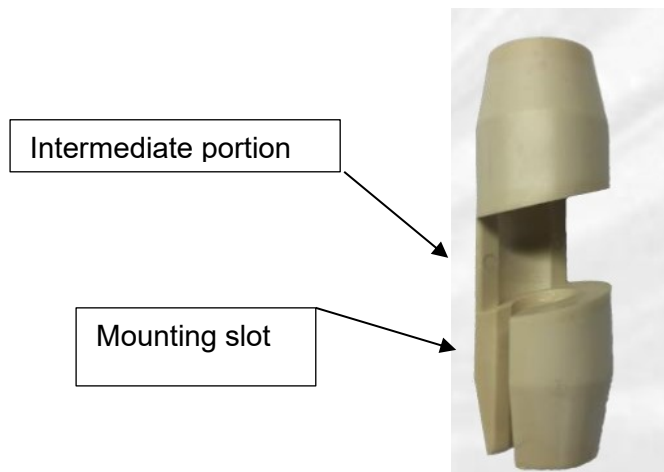
Figure 5 Twisted on rod guide (8)

2) **Slotted design**: this is a cylindrically shaped, longitudinally slotted guide, having tapered top and bottom portions and a longitudinally grooved bore, which is undersized with respect to the rod. The guide has two distinguishable ports, the mouth or entry port which receives the sucker rod initially during the installation, and the exit port which opens to the internal bore of the rod guide.

This guide is installed by placing the entry port of it against the sucker rod, and then striking sharply with a hammer to force the rod guide on the sucker rod. The gripping strength of this rod guide depends on the configurations and materials it is made of.

One of the disadvantages of the slotted design is the likelihood of the rod popping back out during the installation by the operating personnel, and the damage may occur to the rod guide due to repeated mallet blows during the installation.

The beforementioned issues were addressed in literature by using a different design of a slot with different mouth or entry port and exit port configurations as shown in Figure 7. Figure 6 shows the regular slotted design rod guide by Tuboscope.
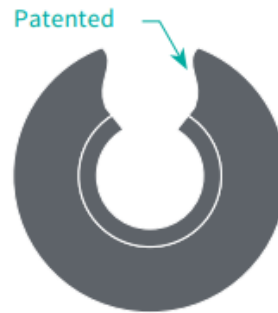

Figure 6 Slotted rod guide (9)

Figure 7 Slot with entry and exit ports (9)

3) **Snap-on design**: this rod guide consists of two identical halves, each half having a tongue and groove that can be snapped together by a sliding slant locking action to form a complete rod guide around the sucker rod.

3.2 Characterisation based on Vane shape

The need for effective paraffin scrapping from tubing wall and reduction of the restrictions of fluid flow in wellbore led to a change in shape and size of rod guides. The first designs for rod guide had cylindrical shape before the vanes came in use. An important parameter in this case is erodible wear volume (EWV) which the amount of material of rod guide that is available for wear before the coupling is subjected to contact with the interior wall of the tubing.

The vanes come in different shapes:

1) **Straight design**: this guide can be described by a cylindrical body moulded on the rod and being coaxial with it. The body carries a plurality of continuous longitudinal vanes, which are integrally moulded on and spaced circumferentially at 90° or 120° angles. The spacing between vanes serves as a flow path for well fluid. Figure 8 shows a straight vane rod guide by Norris.

Figure 8 Straight vane rod guide (8)

This type of rod guides can be extended further with tapered ends to reduce the turbulence.

There are other advantages to be mentioned:

- These guides are cost-effective and long-lasting.
- They provide more bypass volume which results in less resistance for upward fluid flow and fewer drag forces.
- They have a bigger bearing surface (contact between rod guide and tubing)

Disadvantages also exist, such as:

- It does not provide an ideal function for paraffin scrapping unless it is combined a with rod rotator.
- Over time up and down movement of the straight vanes causes grooves in the well tubing.

2) **Slant design**: here, the vanes have angles with the body which removes paraffin from border areas more than straight vane guide. Figure 9 shows a slant vane rod guide designed by Tuboscope.

Figure 9 Slant vane rod guide (9)

3) **Helical design**: many US patents have disclosed this type. The helical vane shape can be described as a cylindrical body with two opposite spiral vanes extended 180° degree. Flow channel is defined and positioned between the vanes. Figure 10 shows a typical helix design.
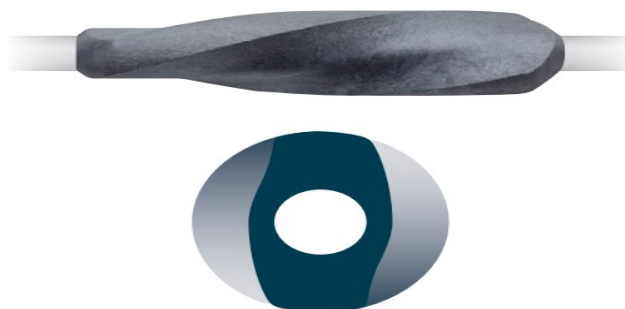
Figure 10 Helical rod guide (10)

In another design, each vane has a forward portion and a backward portion in the same configuration rotating in the opposite direction. It was claimed, that the backward and forward spiralling portions reduce drag forces compared to a continued single vane. (11) (12)

Main advantages of helical rod guides are:

- It provides full paraffin removal circumferentially.
- It eliminates tubing grooving.
- It allows using wide vanes which results in two things; First, increasing contact surface which makes the rod guide tolerate higher side loads and second; more erodible volume. For these reasons, the helical rod guides are more competent in deviated wells.
- It can be used in rotating sucker rods.

One disadvantage is:

- It exerts a torsional force upon the sucker rod.

4) **Wrapping design:** this design is similar to the helical one in terms of spiral vanes and how they oppose each other. Each vane travels 180° degrees around the body. But the difference is in the flow channel which is also defined between the spiral vanes. While the corresponding surface between the vanes in helical design is curvilinear, in wrapping design it is planar. It was claimed the planar surface reduces fluid drag. (13)

The maximum thickness is at the ends, and the minimum thickness is in the middle of the rod guide. Figure 11 shows the wrapping rod guide manufactured by Weatherford

Figure 11 wrapping rod guide (PCT360) (14)

5) **Cylindrical Design:** These designs are meant to be used in reciprocating sucker rod strings. They are active regarding paraffin scrapping because the surface of the vanes is designed in a way that will cover the tubing is internal cylindrical surface.
   a) **Semi-cylindrical vanes:** As shown in Figure 12 which is the isometric view of one embodiment of the moulded-on sucker rod guide, this design consists of a tubular body (18) with two guide portions extended (52 and 50). Each portion is semi-cylindrical with a teardrop shape with side walls (36) and a diameter slightly less than the internal

tubing diameter. The guide portions are inverted and at the widest end have an arc of about 180°. The fluid passageway between the guide portions is shown by (42). while longitudinal cylindrical passageway where the rod should be is shown by (24).
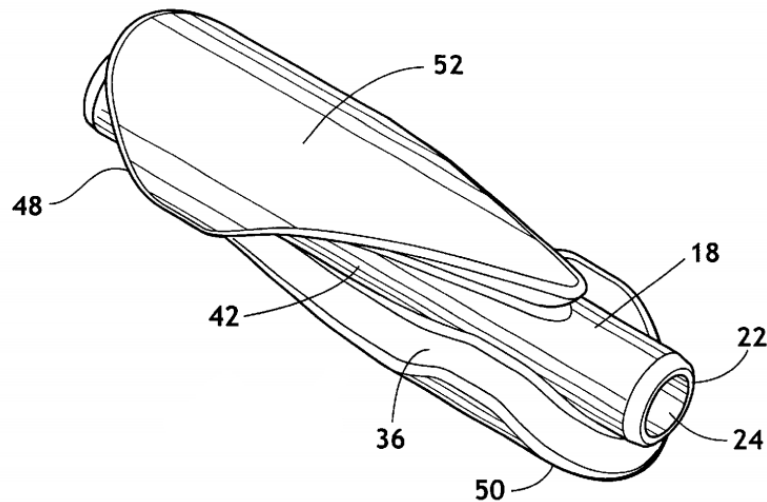
Figure 12 Semi-cylindrical rod guide design (15)

b) Raised ribs vanes:

This guide has sleeves enveloping the sucker rod with raised ribs which are circumferentially arranged to be in contact with the tubing wall.

There are different designs available, and some of them are mentioned below:

- One design is when the ribs are arranged in three diametric planes as it is shown in Figure 13. In the first and the third planes (15, 19) ribs are symmetrically spaced at an angle more than 90° and less than 180° and having circumferential outer surfaces defining a common cylinder. While the ribs in the second plane (17) are in the opposite direction from the middle portion of the sleeve.

  The flow path is defined by the sleeve and ribs (11). The inner bore where the guide can be installed on the rod is shown by (13).

Figure 13 Raised ribs rod guide design (16)

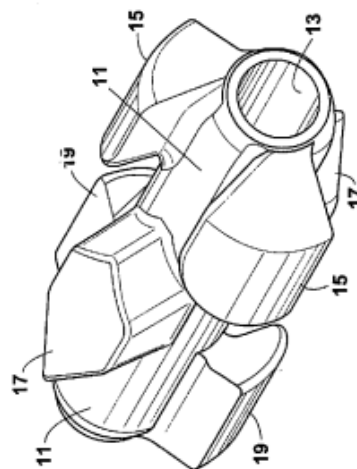- Another design is where three ribs at each end of the rod guide are radially spaced at 120 degrees defining three flow channels between the ribs.

  Each rib has a sharply pointed wedge to scrape and direct material through the flow channel (17). This design was manufactured by Oilfield Improvement Company as it can be seen in Figure 14.

Figure 14 Ultra-flow rod guide by Oilfield Improvement Company (17)

3.3 Characterization based on the movement of the rod string

The movement of the rod sting either reciprocating or rotating, therefore there are two types of rod guides.

3.3.1 Sucker rod pump guides

Many of the beforementioned rod guides are used mainly for reciprocating sucker rods and therefore will not be explained again. But some of them are also employed with a rotating rod string.

However, the optimum rod guide design is for them to be utilised in only for one application.

3.3.2 Progressing cavity rod guides

The rod guide has to protect the rod string from contact with the interior tubing wall without adding much torque on the surface unit that results from frictional resistance.

Another requirement is to have good flow characteristic, to tolerate the solids and adapt to different environmental conditions.

The general components of these rod guides can be described as the following:

- Rotator sleeve which is moulded and secured on the sucker rod. This body is longitudinal and concentric with the sucker rod. It has two stop surfaces at the opposite ends.

- Centraliser or stator sleeve which is slightly larger in diameter than the rotator sleeve and is shorter in length. It can enable the upward and downward movement of the centraliser on the rotator, but this movement is limited by the stop surfaces. Stop surfaces may be constructed from plastic, metal, or similar materials.
- Vanes are moulded to the centraliser with an outer diameter slightly less than the interior diameter of the tubing.

When the centraliser vanes or ribs engage with the tubing, centraliser will stop. And the rotator sleeve will keep rotating with the rod because the frictional resistance between the rotator and centraliser is low. That is why the rotator and centraliser should be made from different material. (18) The centraliser can be moulded, or field-installed with a sleek design like the one known under trademark Seaboard.
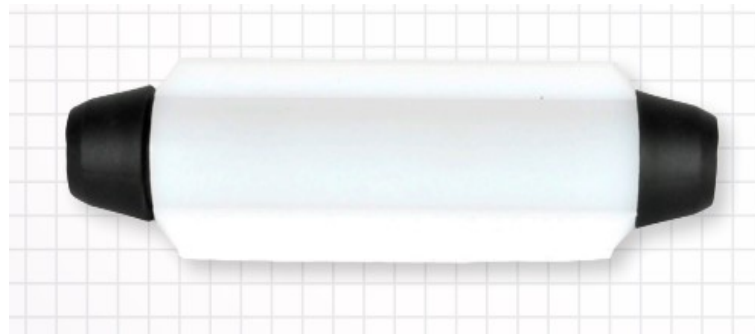
Figure 15 Seaboard (SRC) sucker rod centraliser (19)

Vanes or ribs come with different shapes like the one designed by Tuboscope and shown in Figure 16. The centraliser has three ribs extended outwardly with bevelled end portions at the opposite ends to promote smooth flow profile along the guide. This configuration can reduce the hydraulic resistance and lower the power required to operate the PCP drive.

Figure 16 Spin-Thru rod guide (9)

Vanes designed in a zigzag pattern parallel to the axis of sucker rod was introduced by Weatherford and it was claimed that the zigzag design enables using four vanes with good fluid flow between them without reducing the mechanical strength against shear stress as the sucker rod rotates. This design is shown in Figure 17

Figure 17 SpinTerra ll PCP rod guide (14)

The big challenge for rotating rod guides is sand. The sand causes wear at the interface between the centraliser and centraliser stops. It can also pass through the cavities between the rotator and centraliser from centraliser ends and stop surfaces, which results in reducing the lifetime of the rod guides.

Many approaches to solving this problem were presented. For example, design of vanes in helical shape helps to push the solids out from the space between rotator and stator as it can be seen in Figure 18.

Figure 18 SpinTerra PCP rode guide (14)

Another approach was introduced to harden the interface between the centraliser and centraliser stops by using wafer made of hard material with a hardness value of at least seven on Mohs scale. These wafers can be fixed to the mentioned surfaces so that any abrasives would be crushed and grounded to powder (20).

3.4   Characterisation based on the location of the rod guide

The rod guides can be installed on the shank of sucker rods or the coupling.

3.4.1   Sucker rod guides

All of the rod guides mentioned above are installed on the shank of the rod and therefore will not be explained again.

3.4.2   Rod guides on the couplings

Since the primary purpose of rod guides is the protection of the couplings, the idea of manufacturing couplings with rod guides on them sounds very practical.

3.4.2.1 Rod guide coupling

The rod guide coupling has two threads at opposite ends, and it can connect two successive sucker rods like the regular coupling. But this type has a reduced diameter by about 20% where the guide is moulded on, and the plastic materials can be bound firmly to the coupling (21).

The guides may have different shapes, for instance cylindrical with external flutes defined by grooves between successive flutes. It might also have a cylindrical shape like the one produced by Norris showed in Figure 19. Rod guide coupling can be used preferably in rotating sucker rod strings.

Figure 19 Jake coupling guide (8)

3.4.2.2   Wheeled rod guide coupling

Wheeled rod guide coupling is recommended to be used in the first two or three rods above the pump, first two or three rods below the stuffing box, and wherever there is deviation in the well.

This coupling consists of wheels, which are set in stainless-steel journals and roll pins that are installed in slots angled at 45 degrees to each other along the axis of the coupling as it can be seen from the figure below. (Oilfield Improvements Company)

Figure 20 wheeled rod guide coupling (22)

The wheels roll as the coupling comes into contact with the tubing when the rod string reciprocates. This rolling action can reduce the friction between the rod string and tubing which leads to less power requirement at the surface and increase in mean time between failure. Another advantage of this coupling is that it is easily replaced in fields and it can be changed.

Wheeled rod guide couplings should be used in coordination with the chemical treatment programs because they might be fouled by mineral scale and paraffin deposits, meaning the wheels could no longer rotate.

4 Factors affecting rod guide efficiency

This chapter will discuss the factors that can influence the performance of the rod guide, from the materials and their interaction with the produced fluid to downhole conditions, and the geometry of the rod guide.

4.1 Rod guide materials

Rod guide material is the most influencing factor on the performance of the rod guide. Due to the aggressive environment and fluids that the rod guide is exposed to, the wrong choice of material will lead to deterioration of properties and excessive wear.

The material should therefore have specific characteristics to cope with downhole conditions (pressure, temperature), chemicals, hydrocarbons, side loads and the reciprocating motion of the rod string.

4.1.1 Material type

The preferred materials for rod guides are semi-crystalline thermoplastic polymers because those materials do not soften as the temperature increases. They remain solid until certain quantity of heat adsorbed then they rapidly change to a low viscosity state.
PEEK, PAEK, PPA (AU, AF), PPS, Nylon and PEUHMW are the most popular thermoplastic polymers used in manufacturing of rod guides. (23)
The qualification of thermoplastic materials to be used in oil and gas industry is included in NORSOK Standard M-710.
The mentioned polymers are inherently chemical resistant, wear resistant and have low friction coefficient. But using additives (fillers/extenders, impact modifiers, internal lubricants, reinforcements…) can still change and enhance the polymer properties. (24)

4.1.2 Mechanical properties

Material should have good to high mechanical properties; the higher the better but that can be compromised with the cost.

 In general, mechanical properties can be divided into two groups:

a) **Short-term properties:**
They describe the strength at failure and can be summarized by the following properties:
- Tensile properties.
- Flexural properties.
- Shear properties.
- Compressive strength and modulus.
- Impact strength which measures the ability of the plastic part to adsorb energy and is defined by Izod impact or Charpy impact. It is important to mention that the material should have high impact strength.

b) **Long-term properties:**

They measure time-dependent scenarios like continuous loading or chemical exposure. These effects are presented in the following:

- Creep modulus in tension, flexure and compression.
- Tensile creep rupture.
- Fatigue resistance: since the rod guide is subjected to cyclic stress, the material should have high fatigue endurance.
- Allowable moisture absorption: some materials do not work in high water cut as they have high water absorption at elevated temperature which can affect strength and stiffness.
- The loss of properties due to heat: heat aging and thermogravimetric (TGA) are measurements for the thermal stability of the material.

4.1.3   Thermal properties:

One can distinguish between different measurements:

1) Heat deflection temperature (HDT) which is used to measure the thermal capability under two loads 1.8 MPA (264 psi) and 0.45 MPA (66 psi). It is vital that the material does not work under these conditions.
2) Coefficient of linear thermal expansion (CLTE) which expresses the ratio of the change in length to change in temperature. Rod guide material should have low CLTE. (25)
3) Glass transition temperature (TG): temperature at which the material goes from glassy state to rubbery state followed by properties change like large drop in strength and modulus.

4.1.4   Chemical resistance:

In oil production there are numerous chemicals used as scale inhibitors, corrosion inhibitors, oxygen scavengers, biocide, emulsion breakers, antifoam agents, drag reducing agents, hydrate inhibitors, hydrogen sulphide scavengers, paraffin control agents, asphaltene control agents, etc...

Rod guide material must be compatible with these chemicals. It should operate in high water cut and sour environment in case these conditions are encountered in the well.

Chemicals can affect the material in different forms like adsorption which triggers swelling or extraction some material components by the fluid, causing to weakened rod guide materials. All this will lead to degradation in physical and mechanical properties.

The performance of the material will vary under different conditions like mechanical stress, concentration of the chemicals, time and temperature. (26)

4.1.5 Tribological properties:

The best rod guide material, as mentioned before, is made of semi-crystalline thermoplastic polymer. In sliding applications like the ones rod guides are involved in, it is vital to choose the right type of polymer, and that is high temperature polymers because they can resist the frictional heat (23) .

The tribological properties can be presented by the following:

A. **Wear:** polymer wear can be in the form of adhesion, abrasion or surface fatigue. Polymer wear rate will define the lifetime of rod guides. in other words, the required time for erodible wear volume (EWV) to be consumed.
   The lower the wear rate, the longer the service life of the rod guides which is the ideal case to extend MTBF.
B. **Friction:** the friction coefficient is the division of friction force to the normal applied load. It can be either a static or a kinetic friction coefficient. The material should have low friction coefficient because lower friction forces means lower energy consumption.
   The wear and friction are controlled by many factors:
   1) **Material:** Wear and friction are influenced by mechanical, physical and thermal properties. Some polymers are inherently wear resistance. Using some additives (e.g. PTFE–Polytetrafluoroethylene (10-20%), Silicone–Polydimethylsiloxane (1-3%), Graphite Powder (5-15%) and Molybdenum Disulphide–MoS2 (1-5%). and reinforcements (e.g. Glass Fibre (5-50%), Carbon Fiber (5-50%) and Aramid Fiber (5-20%), one can enhance the wear resistance and friction
   2) **Geometry:** Since the rod guide is produced by a process called injection moulding, the plastic shape will introduce some stress concentration (if the guideline design of the plastic part was not taken into consideration) that leads to decrease in the mechanical properties. For example, the impact strength, which is the ability of plastic part to adsorb energy, is a function of the of the shape, size, thickness, and the type of plastic. By decreasing the mechanical properties, the wear resistance will decrease (25).
   3) **Produced fluid**: Since fluid acts as an external lubricant, it will influence the wear and friction in different ways. Different fluids exist within the wellbore, such as:
      - Water cut: wear and friction is better handled in an oil lubricant than in water.
      - Chemicals: they accelerate the wear by a process called corrosive wear where first the chemicals attack the surface then the sliding movement corrodes this layer to be replaced with a fresh one.
      - Sand: the abrasive wear might increase in the presence of sand, that is why some polymers cannot operate in sand service.
   4) **PV:** Where P stands for the average contact pressure and V the sliding speed. Every polymer has a PV limit which should not be exceeded because after this limit, severe wear will occur.

5) **Wall tubing roughness:** The decrease in roughness causes a decrease in friction coefficient and wear rate until a certain value. Afterwards, more decrease in the roughness leads to higher wear rate.

4.2 Rod guide Geometry

There are certain considerations in the geometry of rod guide in order to achieve the best performance. The following is the list of properties that define proper rod guide:

- **Good Bypass:** this means the cross-sectional area where the fluid flows through the rod guide. If this cross-sectional area is small, the rod guide will serve as a restriction point and causes reduction in the production rate.
- **Less turbulence and drag resistance:** the geometry of the rod guide should provide smooth flow paths close to laminar because the higher the turbulent flow the higher the drag coefficient.
- **Erodible wear volume (EWV):** EWV is an important indicator of rode guide performance and defines the lifetime of the rod guide. The rod guide should provide acceptable EWV without sacrificing the two properties mentioned above. (27)

4.2.1 Rod guide Surface description

There are different surfaces in the rod guides to be identified:

- **Wear surface**: This is the surface of each vane where it contacts with the interior wall of the tubing
  Rod guide will have different wear surfaces depending on the number of vanes. It might be three, four, or even two. Obviously, the bigger wear surfaces of the rod guide provide better scrapping effect, but this is not ideal for fluid bypass.
- **Leading surface:** Every rod guide has tapered ends to reduce the turbulence and drag friction of the fluid, the leading surface which can be planar or curved is the surface that connects the tapered end with wear surface.
  The purpose of the leading surfaces is to provide smooth flow of the fluid over the vanes and the passageways between the vanes as well.
- **Side wall surface:** Every two side wall surfaces define one vane. This surface can be planar or curved.
- **Surface between the vanes:** The fluid flows over the vanes and through the channels which are defined by two wall surfaces from different vanes and bottom surface.
  The edges between all the mentioned surfaces should be rounded for further drag reduction. The degree of rounding depends on manufacturing convenience.

4.2.2   The length and Diameter of the rod guide

These are important parameters to reduce the turbulence and drag coefficient. Rod guide diameter is typically is slightly less than the tubing inner diameter. The best ratio L/D found in literature, for straight guides (chapter 3) to decrease turbulence and drag coefficient is between 2.1 and 3. (28). However, some companies like RFG produce rod guides that have a higher ratio.

5 Design of a protector for wire rope activated pump

This chapter will go through the design of a rod guide or protector for wire rope activated pump using Solidworks software, and explains the considerations that were taken in.

5.1 Protector description

The protector was designed for a pre-stressing stranded wire rope which is manufactured by Voestalpine (Figure 21). The wire rope is a 15.7 mm stranded non-alloyed carbon steel consisting of 7 wires, each with a diameter of 5 mm. The wires have a zinc coating which accounts for 0.7 mm and are covered with wax to reduce friction between them while movement takes place.
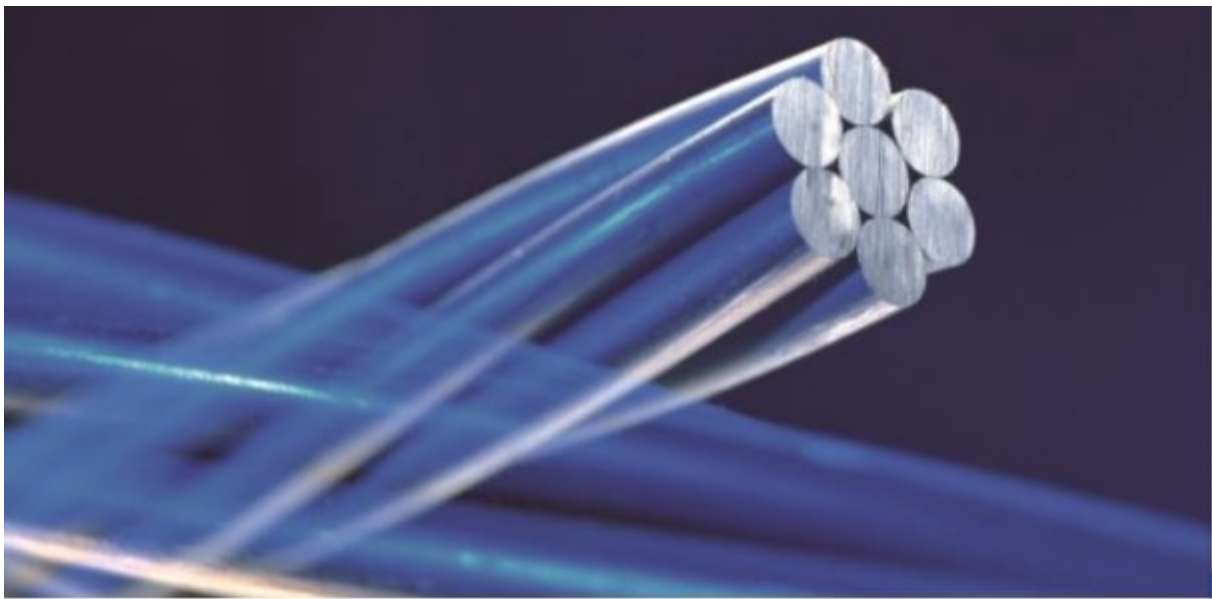

Figure 21 Pre-stressed stranded wire rope (29)

The protector was constructed using surface modelling in Solidworks which appears to be the best way to make smooth surfaces. Some considerations regarding the guidelines to injection moulding process must be in place when constructing plastic parts, like using uniform wall thickness, avoiding sharp edges and others. Guidelines differ from material to material, however, all guidelines intend to avoid stress concentration and mould filling problems.

The protector is made of two identical parts placed by snapping and sliding action of the two parts on the cable. The protector consists of a cylindrical body concentric with the cable and four ribs defining a common cylinder with almost 360° scrapping effect.

Figure 22 shows the protector in assembly with the wire rope with different surfaces as explained before. From the same figure, it can also be seen that the protector has four ribs located in two planes perpendicular to each other, where on each plane, the two ribs extend radially outward from the cylindrical body and they are positioned symmetrically in opposite direction to each other.
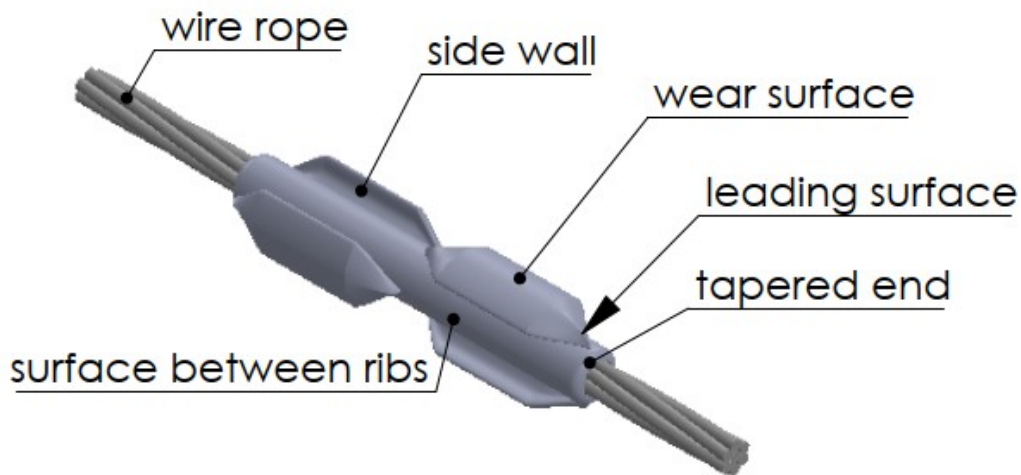
Figure 22 Protector in assembly with the wire rope

The internal surface of the protector can be made in a way to match the configuration of the wire rope which can increase the holding grip of the protector on the wire rope, but this might complicate the design of snap-fits. For this reason, the internal surface of the protector was made cylindrical.

The idea behind this design is that in a wire rope activated pump, unlike the conventional sucker rod pump where the sucker rod string is being rotated from the surface by a rod rotator to provide uniform circumferentially erosion, the cable cannot be rotated to provide this uniform erosion.

5.2 Protector assembly

Protector is constructed in two identical parts that can be mounted on the cable by pressing and sliding action. As it can be seen in figure 23, each part has a lip and a groove, the lip from each part intersects with the groove from the other part through sliding action. In addition to the lip and the groove, each part is provided with a cantilever beam and locking feature. In the same manner as for the lips and the grooves, each cantilever beam from one part intersects with the lock feature from the other part. This way the protector can be installed onto the cable first by pressing the two protector parts laterally against the cable as it can be seen in figure 24.Second sliding action is performed when each lip from each part intersects with groove from the other part and in the same manner, each cantilever from each part intersects with the locking feature from the other part figure 25.
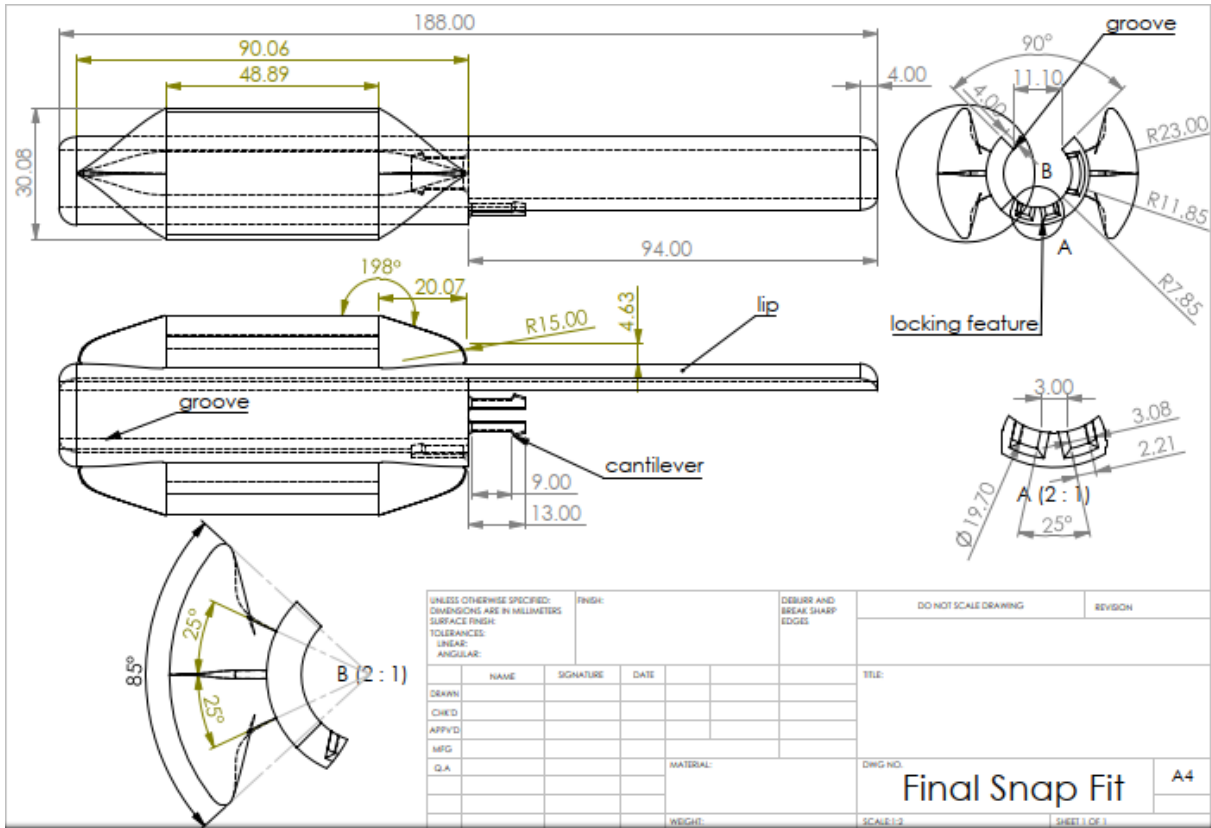
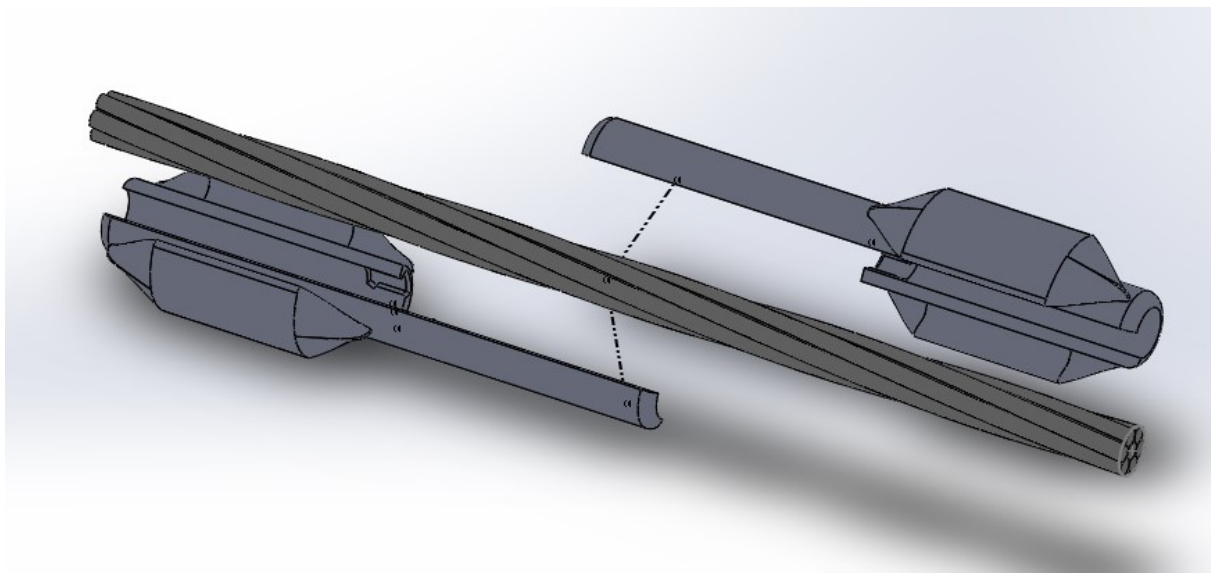Figure 23 Drawing of protector part
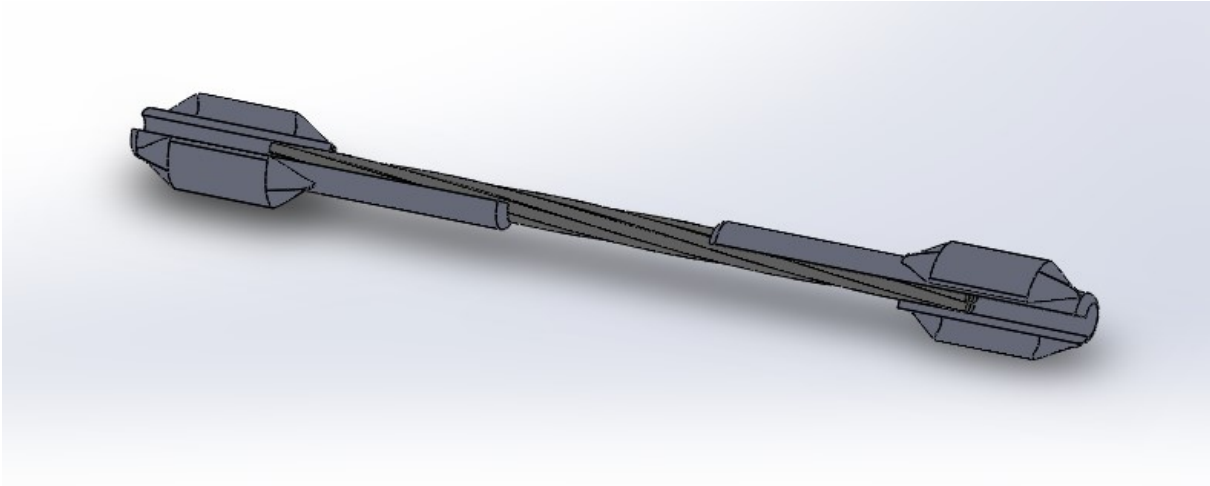

Figure 24 Two parts in pressing action

Figure 25 Two parts in sliding action

5.3 Holding grip

Since the protector is not moulded on the wire rope, the holding grip for the protector on the rope is an issue. For some designs, like slotted and twisted-on design, the insert metal can improve the holding grip but there are issues regarding corrosion. On the other hand, designs where the protector consists of two parts that can be assembled on the wire rope or sucker rod, which the case for the current design , the issue is how the two parts can hold to each other and provide enough contact pressure for the protector on the wire rope or sucker rod to prevent slipping.

5.3.1 Interference fit calculation

The clearance between the wire rope and protector which determines whether the two parts move independently or are permanently joined, is called "fit" and there are different types of fit:

- Clearance fit: The hole and the shaft can slide and / or rotate in assembly because the hole is larger than the schaft .
- location/transition fit: The hole is fractionally smaller than the shaft and mild forces are required to assemble / disassemble.
- Interference fit: The hole is smaller than the shaft and high forces and / or heat are required to assemble / disassemble. This type is used to determine the tolerance range for the inner hole of protector

For interference fit, the maximum admissible force between the protector and the wire rope should be bigger than the value to fit the wire rope and protector. The material that was used for the interference fit calculation is shown in the appendix A.

The maximum compressive force applicable from the protector on the wire rope is equal to the surface area (the surface area of the hole of the protector) times the compressive strength of the protector material.

$$F_{MAX} = 9273 * 23 = 213.2 \text{ KN}$$

The maximum pressure force that can be applied to the protector is given by the formula

$$P = {F_{ax}.S_r}\big/{(\pi.D_{F.}.l.\mu_r)}$$

Equation 1 Pressure contact between parts (30)

F_{ax} is the maximum axial force, Sr is safety factor 1.2, D_F is the diameter of the hole 15.7mm, l is the length of protector 188 mm, μ_r is the coefficient of friction between the material and steel. The maximum pressure between the wire rope and protector is equal to the compressive strength so we can get the maximum axial force from the equation 1 (F_{ax}= 44.4 KN). From the axial force the normal force can be calculated where the normal force is the axial force divided by the coefficient of friction

Fn= 44.4/0.25=177.6 KN as it can be seen the Fn < Fmax.

ISO system uses numeric codes to define the tolerance range for the fit, the upper case to represent the hole tolerance and the lower case to represent the shaft (wire rope) tolerance.

The DIN ISO 286 was therefore used to determine the tolerance of the hole since the tolerance for the wire rope is already known. The tolerance for one strand in the wire rope is 1/200 mm and for the wire rope is 0.03 mm, therefore based on standard "r6" for the tolerance of the shaft (rope), the upper tolerance should be 0.034 mm and the lower tolerance should be 0.023 mm. The used standard for the tolerance of the hole (protector) is "H7", according to which the tolerance should be between 0 and 0.018 mm. The maximum interference is 0.034 mm and the minimum is 0.005 mm.

The pressure contact can be calculated by the following formula:

$$P = \frac{I}{\frac{d}{E_0} * \left[\frac{d^2{}_0 + d^2}{d^2{}_0 - d^2} + V_0 \right] + \frac{d}{E_i} * \left[\frac{d^2{}_i + d^2}{d^2{}_i - d^2} - V_i \right]}$$

Equation 2 Pressure of contact between Hub and shaft (30)

The values for the mentioned parameter can be seen in table 1. The maximum pressure generated at interference 0.03 mm is 1.45 Mpa and minimum pressure is 0.25 Mpa.

The minimum axial force to engage/disengage or the friction force is 0.58 KN at minimum interference 0.005 mm and 3.45 KN at interference 0.03 mm.

Parameter	Value	Unit
Hub young's modulus E_0	3.8	GPa
Hub Poisson's modulus V_0	0.378	
Shaft young's modulus E_i	187	GPa
Shaft Poisson's modulus V_i	0.3	
Compressive strength of used material	23	Mpa
outer hub diameter d_0	19.7	mm
nominal rim diameter d	15.7	mm
Coefficient of friction between steel and the material μ_r	0.25	

Table 1 Parameter of input equation2

5.3.2 Snap-fit calculation

The cantilever beam was constructed based on the recommendations of The First Snap-fit Handbook (31). As it is shown in Figure 26, the parameters for the beam in the current design are the following: b =10 mm, h= 2 mm.

First, the permissible deflection is calculated by the following formula:

$$y = 0.67.\varepsilon.b^2/h$$

Equation 3 permissible deflection

Where ϵ is the yield strain at the design point. For unreinforced plastic, it is 70 % of the yield strain and for reinforced plastic 50 % (32). The material used in the current calculation is in Appendix A. yield strain is 5% and the material is unreinforced so ϵ= 0.035. Permissible deflection or permissible undercut is therefore 1.17 mm. The undercut must be below this value. y was chosen to be 1 mm.

Next step is to calculate the deflection force P in Figure 26

$$P = (w.h^2.E_s.\varepsilon)/6.b$$

Equation 4 deflection force (32)

Where E_s is secant modulus. E_s =2500 Mpa from the material properties at yield strain 0.035. deflection force is therefore equal to 11.66 N
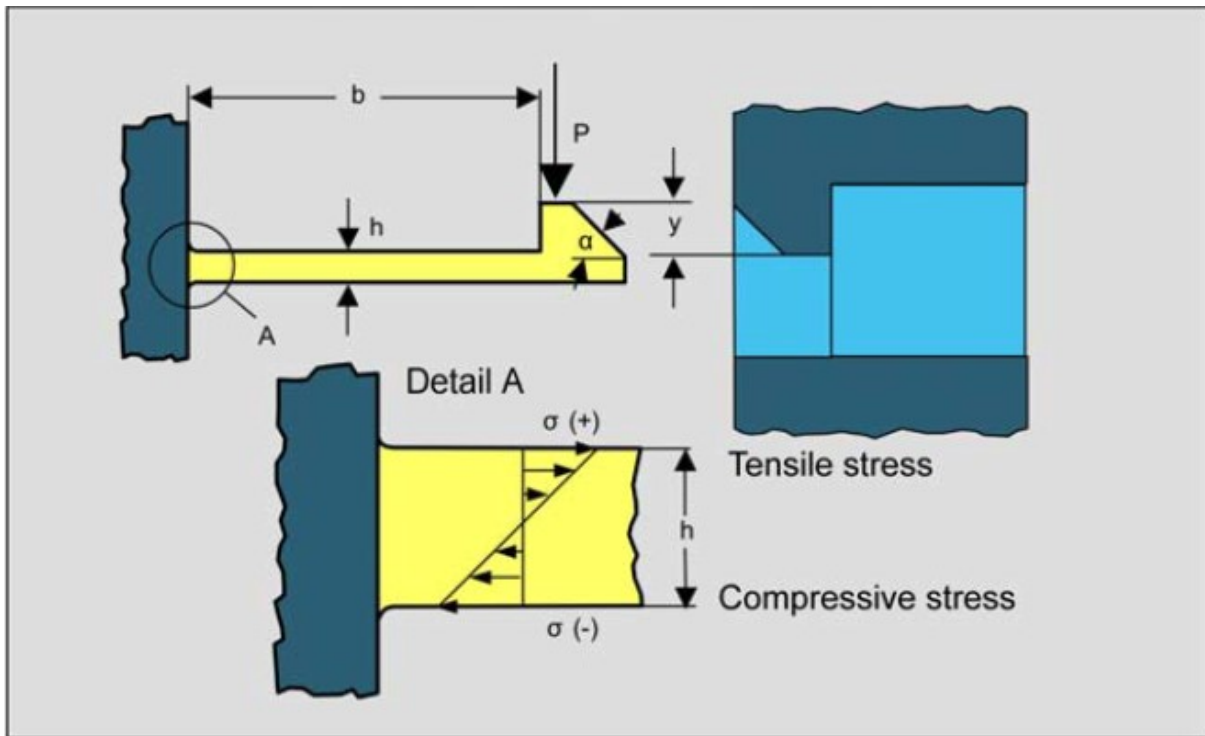
Figure 26 simple cantilever snap (32)

The assembly force is later calculated by the following formula:

$$F_{assembly} = P \frac{(\mu + \tan a)}{1 - (\mu . \tan a)}$$

Equation 5 Assembly force (32)

Where α is the insertion face angle (Figure 27) was chosen as 20° to decrease the assembly force, P is the deflection force and μ is the coefficient of friction 0.4. Assembly force for one snap-fit is then 10.35 N.

For separation force, the retention face angle must be above 45° and below 90°. At 90° the snap-fit will be permanent. Hence, the threshold retention face angle must be calculated at the beginning because at this value the snap-fit will behave as 90°.
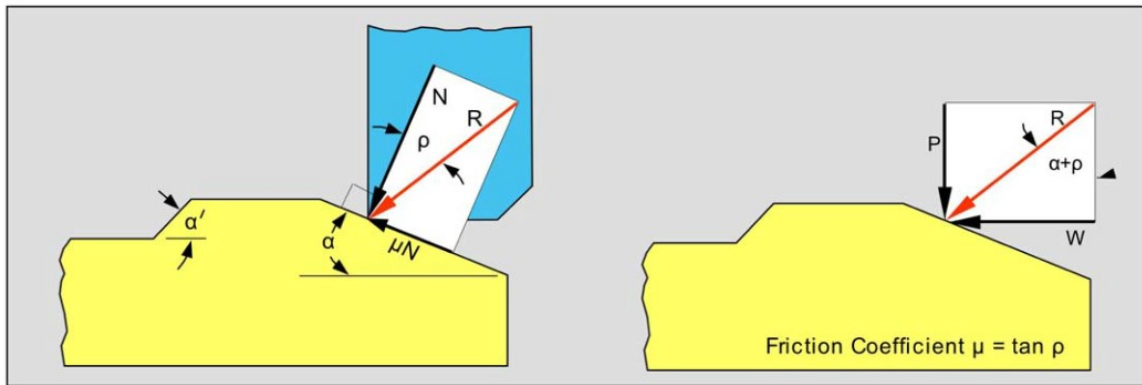
Figure 27 insertion face angle and retention face angle

The threshold angle is function of the coefficient of friction

$$\alpha'_{thershold} = tan^{-1}\left(\frac{1}{\mu}\right)$$

Equation 6 Threshold retention face angle

The threshold angle is 68°, therefore the retention face angle was chosen to be 60

The separation force is calculated with the same formula in equation 5 after replacing α with α'. The separation force for on snap-fit is then 80.6 N. The force needed to separate the four snap-fits, is therefore 322.2 N.

The total forces needed to separate the two parts includes the separation forces for four snap-fits in addition to friction forces between the lips and grooves and the friction forces between the wire rope and the internal surface of the two parts as well.

6 Flow simulation

The flow simulation was performed in Ansys Fluent which allowed the modification and improvement of the rod guide mentioned in the previous chapter. The main purpose of the simulation is to decide on the best protector that provides less pressure drop and acceptable erodible wear volume

6.1 The governing equation

The flow in the tubing around the protector is a turbulent flow, so a turbulent model must be used. Choosing the right turbulent model for successful CFD simulation, depends on the nature of the problem.

However, there are different types of turbulent models, each one having its limitation and advantages. The turbulent model that was used in this simulation is the "SST k-ω" turbulence model because this model shows highly accurate predictions of the flow separation.

SST k-ω is a two equation model for the turbulence kinetic energy (k), and turbulence specific dissipation rate (ω), that combines k-ε model in the free stream and the k-ω model in the inner region of the boundary layers, using the Low-Reynolds-Number method to resolve the details of the boundary layer which can be achieved by using very thin inflation layers near the walls.

6.2 Geometry

After importing the geometry from Solidworks in STEP format, the fluid domain was constructed in DesignModler Ansys fluent 18.2 with length of 1 m where the distance from the centre of the protector to the inlet and outlet is 0.5 m. For meshing purposes, the fluid domain was divided in three parts as shown in the figure 29. Different geometry models were prepared for the purpose of parametric analysis so that the model that provides less pressure drop, drag coefficient and acceptable erodible wear volume will be chosen. The main parameters that was changed was the cross-sectional area of the protector occupied the selected diameter. This was achieved either by changing the diameter of the tubing or the shape of the vane, and the second parameter was the length of the protector which would increase the surface area in contact with fluid.

Table 2 below shows the different parameters for each constructed fluid domain, the length of the protector, diameter of protector which is constant for all models, cross erodible wear volume, the inside diameter of the tubing, surface area of the model that is in contact with fluid, and the cross-sectional area expressed as a percent of the area encompassed by the selected tubing inside diameter. The geometry that was described in chapter 5.1 is used in simulation 4.

The difference between the geometry used in simulation 1 (appendix B) and 4 is the shape of vanes. The width of the bottom of the vane for Simulation 1, where it is connected to the cylindrical body, is 16.01 mm, while in Simulation 4 (figure 28) is 10.03 mm.

For simulation 2, the geometry is the same as simulation 1 but the diameter of the tubing is increased. The geometry in simulation 3 has the same shape of vane as the geometry in simulation 1 but the length of the protector was increased.
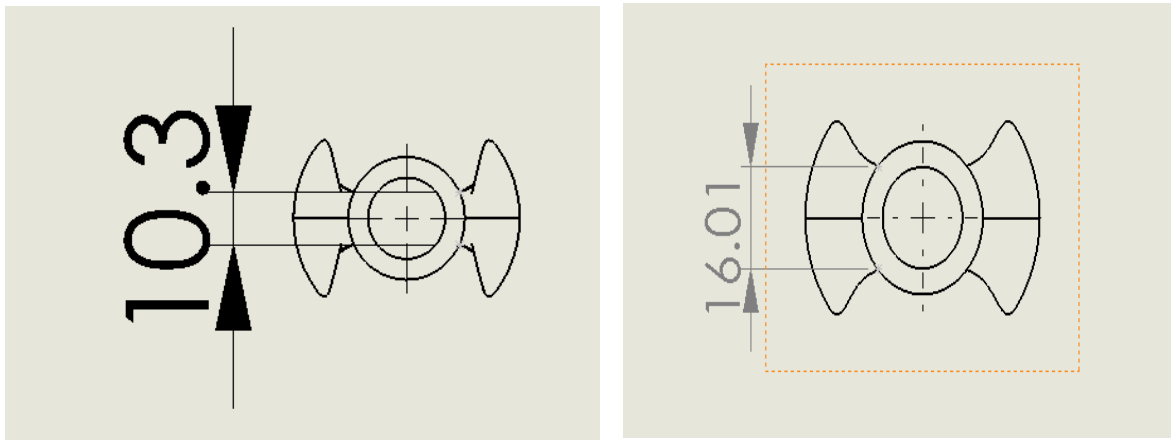

Figure 28 Simulation 4 left, simulation 1 right sketch shows frontal view of two ribs
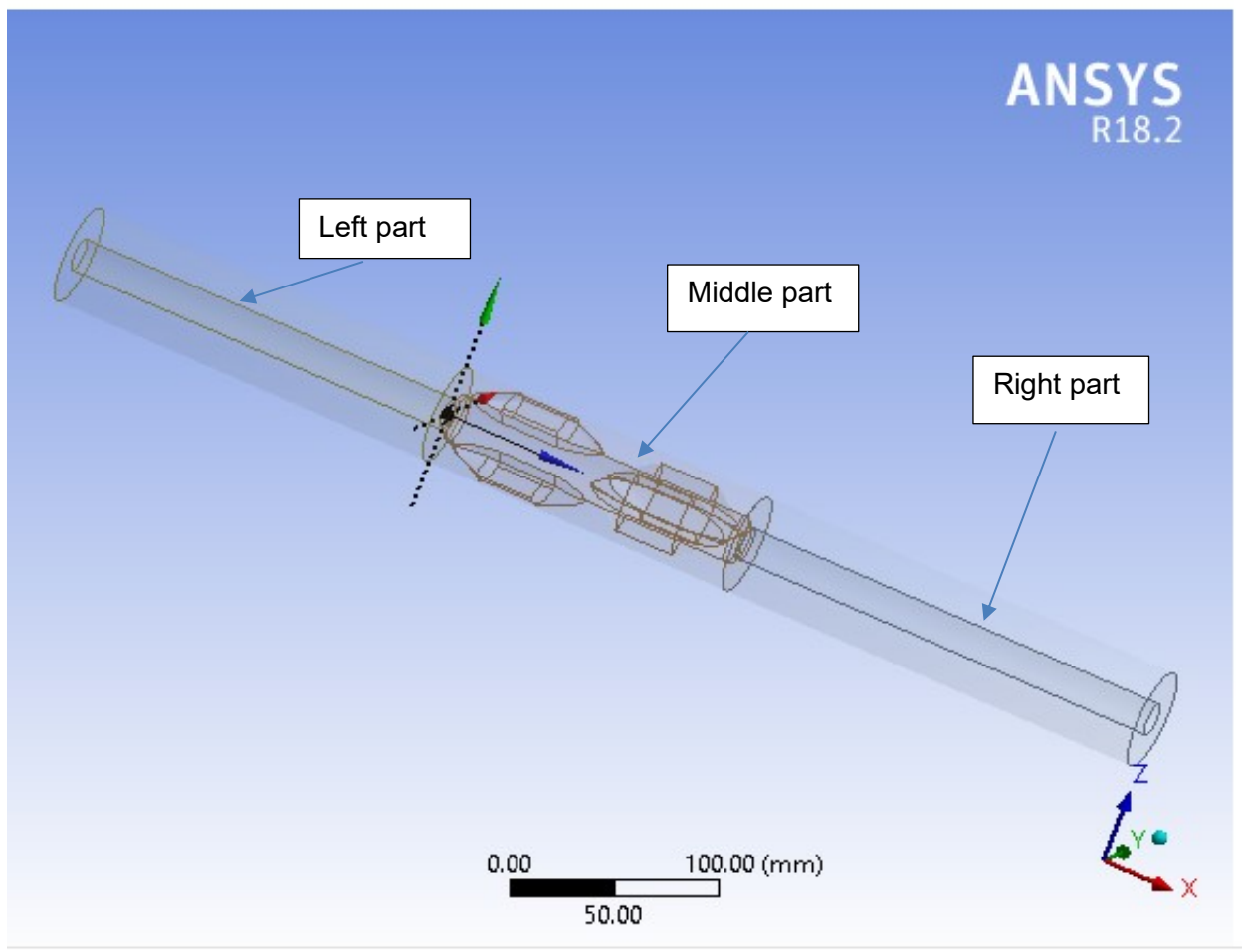

Figure 29 Fluid domain in DesignModler

Simulation	Length (mm)	Diameter (mm)	Cross EWV (cm³)	ID Tubing (mm)	Cross-sectional area (%)	Surface area (m²)
Simulation 1	148	46	51.52	50.673	49.36	0.0193
Simulation 2	148	46	51.52	51.8414	47.16	0.0193
Simulation 3	168	46	62.56	50.673	49.36	0.0269
Simulation 4	188	46	59.48	50.673	44.36	0.0284

Table 2 Parameters of the models

6.3 Meshing

It is a challenging task in CFD to find out the right mesh for the simulation, because the solution will differ depending on the mesh resolution. Meshing is an iterative process, there are some steps that can help to define the right mesh as they are explained in the following:

- Checking the mesh's orthogonal quality, aspect ratios and skewness. The ideal solution is to maintain the best mesh quality as much as possible because a bad mesh quality will cause divergence problems affecting the solution accuracy.
- The solution must be converged. Convergence means that the residual errors value which measures the local imbalance of a conserved variable in each control volume, should drop below certain value. The residual level was set to 1E-4. There is another criterion to judge the convergence which is through monitoring of some variables like average weighted value of the static inlet pressure. At a converged solution, the monitored variable value should be constant.
- The match between the simulation results and the experimental data.
- Grid independence study, where further refinement of the mesh will result in small changes for the chosen calculated variable.

A hybrid mesh from hexahedral and polyhedral shape is used in this simulation. The tetrahedral cells were first generated on the middle part of fluid domain with "Patch Conforming Method", then they were converted to polyhedral to reduce the number of elements while the hexahedral cells were generated on the right and the left part with "Multizone methods". In addition, to face and edge sizing was implemented to improve the mesh quality.

The inflation layers which are very important to capture the physics near the walls, were generated on the internal wall and pipe wall for a total thickness of 0.0004 m and with a number of 5 inflation layers.

6.4 Model setup

The following explains the model setup inputs:

A. **Model**: The case of study has turbulent flow of water in steady state. As mentioned before the model set to perform this simulation was SST k-ω.

B. **Boundary conditions**: choosing the boundary conditions is another essential factor for successful flow simulation. Since the pressure drop is meant to analyse, the boundary conditions were assigned as the following:

- The Inlet velocity in the x direction with value 0.79 m/s (figure 30).
  The turbulence specification factors are intermittency, turbulent intensity and hydraulic diameter. Intermittency is a factor introduced in the source term of the ST turbulent model where intermittency=0 is in laminar flow, 1 is in turbulent flow and for transition, it takes a value between one and zero.
  The turbulence intensity is calculated by the correlation

$$I = 0.16\, R_H{}^{-1/8}$$

Equation 7 Turbulence Intensity (33)

And Reynolds number is:

$$R_H = \frac{\rho V D}{\mu}$$

Equation 8 Reynolds Number (33)

Where density ρ= 998.2 kg/m³, viscosity μ= 0.001003 kg/m-s, hydraulic diameter D=0.035 m which is the tubing diameter minus the wire rope diameter and velocity v=0.79 m/s.
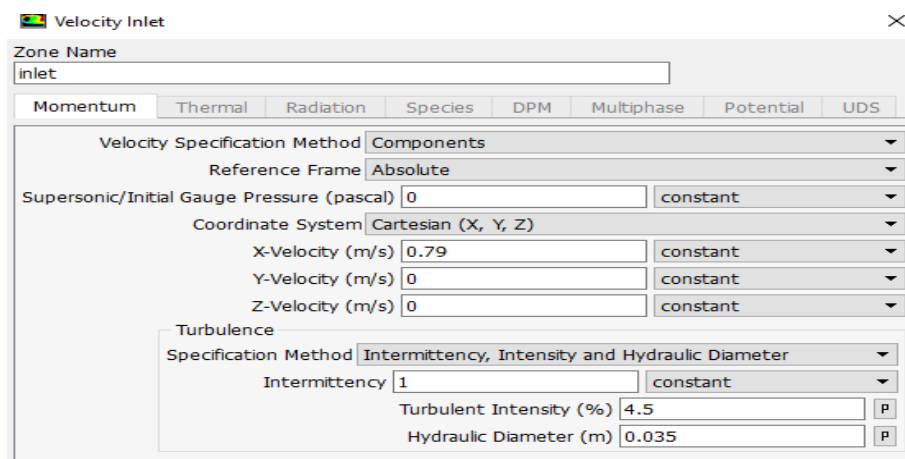

Figure 30 Inlet boundary condition

- Walls which can be divided into stationary wall named as pipewall and moving wall named as innerwall. The moving wall represents the wire rope with the protector. Both

walls are no slip walls and the roughness is set to be zero which means they are smooth pipe.

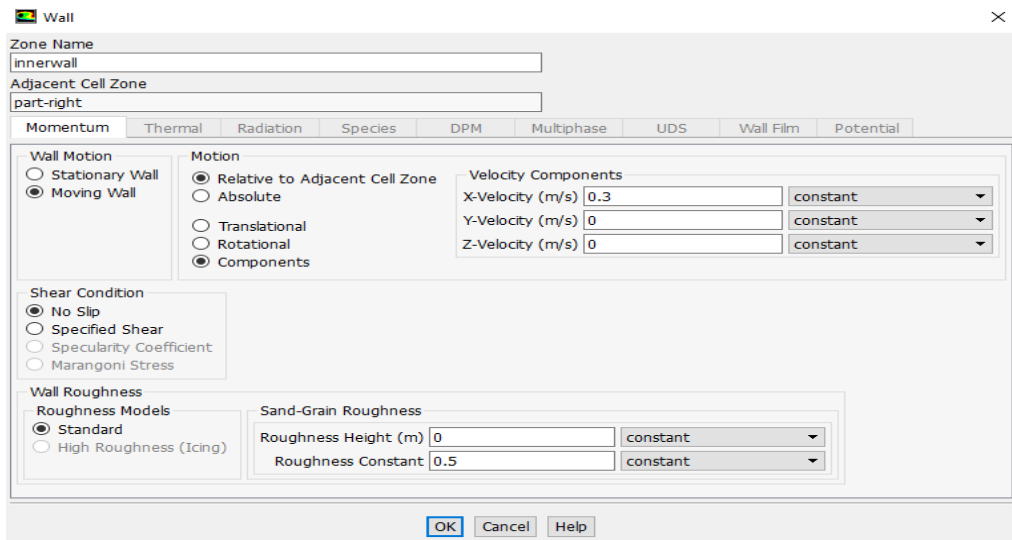The velocity of the moving wall is set in the X direction with value of 0.3 as it can be seen in figure 31

Figure 31 Moving wall boundary condition

- The outlet pressure with gauge pressure set to zero.

C. **Solution**: used solver is a pressure-based segregated solver with scheme SIMPLEC algorithm. Pressure-based segregated solver is applicable for wide range of flow regime and requires less memory than other solvers.

For spatial discretization, PRESTO is used for pressure and the rest (momentum, turbulence kinetic energy, specific dissipation rate, intermittency, momentum thickness Re) is set on Second Order Upwind to provide more accurate results.

D. **Initialization:** for starting the calculations, the flow field in the entire domain must be initialized. The field flow was initialized using standard initialization with values set for the inlet. Once the inlet is selected from "Compute from" drop-down list, all the values under "initials values" will be automatically generated based on the inlet condition.

6.5 Verification

Verification determines if the computational implementation of the conceptual model is correct. Verification assessment involves a grid independence study which is meant to estimate the discretization error of the numerical solution. When the variable of interest doesn't change with the finer mesh, the solution is independent of mesh size, hence the discretization error should approach zero. The variable of interest was the static input pressure since the pressure drop is intended to be analysed (the pressure drop is the inlet pressure minus the outlet pressure (outlet pressure is zero). Mesh independence study was carried out for all the simulations.

Iterative convergence, which is another task that involves verification assessment should be also done, where the residual error level must drop to a specified value in which the static inlet pressure doesn't change with more iterations. The residual error level is set to be 10E-4.

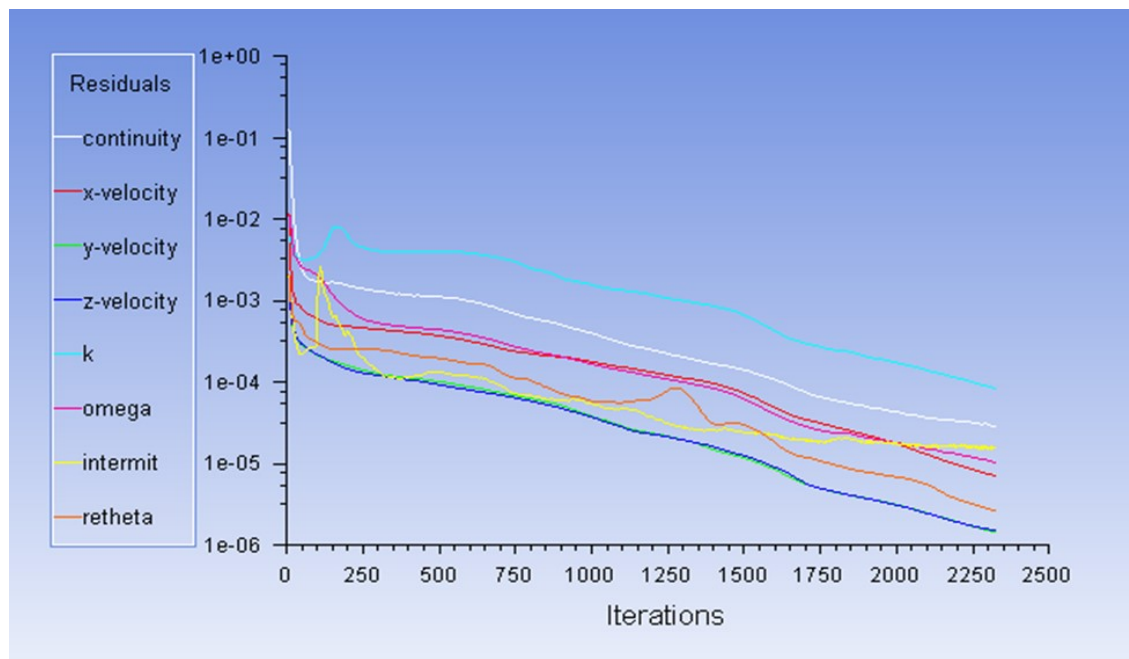Figure 32 show the residual errors for geometry 4 presented in table 2.

Figure 32 Residuals for model 4 simulation

6.6 Validation

Validation is the process of determining the accuracy of representation of the model to the problem in reality. The validation was carried out by running the simulation for the rod guide that was disclosed in the patent US 5115863, then comparing the results of simulation to the results from model 1 and 4. The rod guide is described as a cylindrical body that carries four longitudinal vanes spaced circumferentially at 90° angles. The body is coaxial with the sucker rod and tapered at each terminal end to minimize the fluid drag. The dimensions of the rod guide and drag coefficient as mentioned in the patent are presented in Table 3.

The rod guide was reconstructed in Solidworks as it can be seen in Figure 34 and the two geometries in simulation 1 and 4 were scaled to be used in a 63.5 mm tubing diameter and match the reconstructed rod guide as much as possible for the sake of comparison. Table 4 shows different parameters for the reconstructed rod guide and the scaled geometries 1 and 4.

Tubing diameter (mm)	Cross-sectional area (%)	Diameter (mm)	EWV Cm³	Length mm	Drag coefficient for fluid velocity 0.79428 m/s
63.5	56.6	59.055	62.92633	127-177.8	0.63

Table 3 Parameters of the patented rod guide (28)

For calculating the drag coefficient in Ansys the reference value must be defined, hence the drag coefficient is calculated by the following formula:

$$C_d = \frac{D_f}{\rho\, A\, V^2/2}$$

Equation 9 Drag coefficient (34)

Where D_f is drag force in the direction of flow velocity, V is the velocity and A the projected area of the protector normal to the flow velocity and ρ is the density. The following figure 33 shows the reference value in Ansys.

Figure 33 Reference value scaled geometry 4

Geometry	Length (mm)	Diameter (mm)	EWV Cm³	Cross-sectional area %	Fluid-contact Surface area (m²)
Rod guide	170.31	59.06	3.84	56.6	0.0304
Geometry 1	170	61.59	4.03	56.6	0.0291
Geometry 4	175.67	61.18	3.66	50	0.0334

Table 4 Parameters of the reconstructed rod guide and scaled geometries 1 and 4
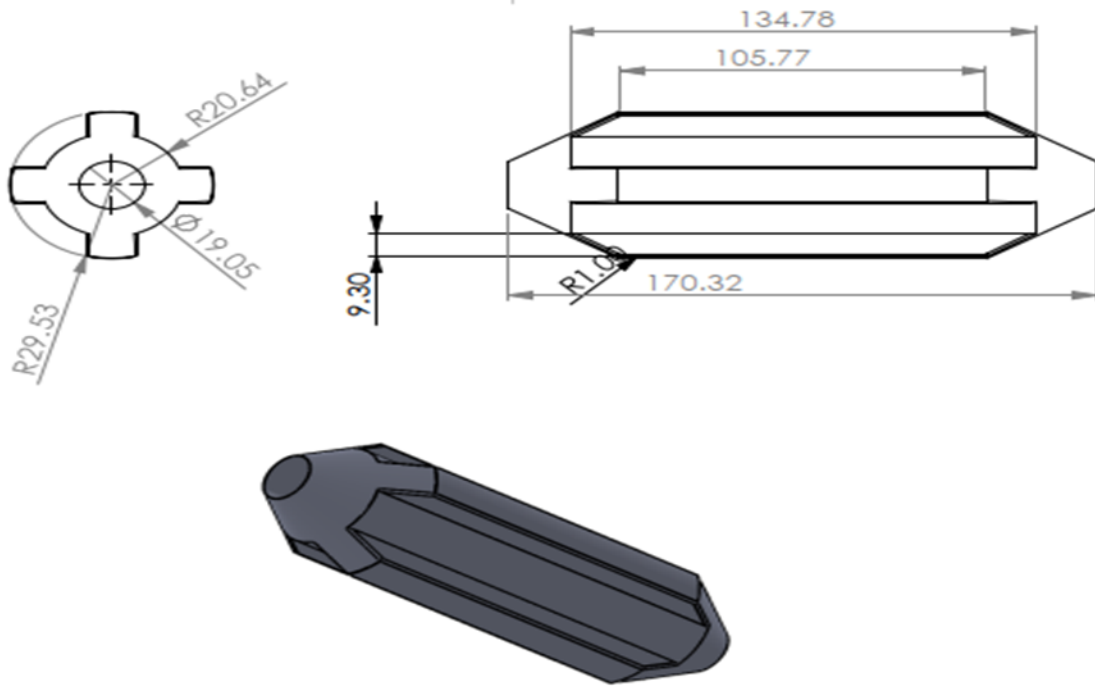
Figure 34 Reconstructed rod guide

The result of drag coefficient for reconstructed rod guide from the simulation shown in Table 5 is 0.68 which is 7.35 % more than the result presented in the patent shown in Table 3.

Geometry	Drag coefficient
Reconstructed rod guide	0.68
Scaled Geometry 1	0.77
Scaled Geometry 4	0.60

Table 5 Simulation results of drag coefficient

7 Results and discussion

This chapter introduces the simulation results of the models and discusses the reason behind choosing the model presented in chapter 5.

7.1 Drag coefficient

The basic drag force consists of the drag form or what is called the pressure drag, which is a function of the body shape and the flow separation, and the frictional drag which is a function of the boundary layer properties (roughness). The drag force acting on an immersed body is presented in the following equation:

$$D_f = \int_A P \, \sin\theta \, dA + \int_A \tau_0 \cos\theta \, dA$$

Equation 10 Drag force

Where P is pressure, θ is the angle of attack, τ_0 is the shear wall stress, and A is the surface area.

Drag coefficient is the ratio of the drag force to the force produced by dynamic pressure times area and it includes the skin friction (it comes from frictional drag) and the shape (form) (it comes from pressure drag), therefore drag coefficient depends on the shape, inclination and flow conditions.

In the validation process conducted in chapter 6, the reconstructed rod guide and geometry 1 had the same surface area but a different shape, as it can be seen in table 4, which means the drag form of the drag forces will have the main contribution in the total drag coefficient value.

Table 5 shows higher value for drag coefficient for scaled geometry 1 than the reconstructed rod guide while the drag coefficient is the least for scaled geometry 4.

The results also show the reduction of the cross-sectional area occupied by the geometry ill reduce the drag coefficient.

7.2 Erodible wear volume and pressure drop

Pressure drop can be calculated by a general formula

$$\Delta P = f.l.\rho.u^2/(D.2)$$

Equation 5 Pressure drop

Where l is the length of domain, ρ is the density, u is the main velocity, D is the hydraulic diameter and f is the friction factor which is a function of Reynolds number and dimensionless roughness and it can be determined experientially for turbulent flow.

The difference between simulation 1 and 2 is that the tubing diameter for simulation 2 is bigger which means the hydraulic diameter is higher and the higher hydraulic diameter is, the higher the Reynolds number. For higher Reynolds numbers, the friction factor is less. According to equation 5, this will result in less pressure drop as shown in table 6.

For simulation 3, the geometry is the same as simulation 1 but the length is longer which means the pressure drop should be higher according to equations 5 again.

In Simulation 4, the geometry was constructed to occupy less cross-sectional area than the geometry in simulation 1, 2, and 3 for tubing diameter 50.673. Although the length of the protector in simulation 4 is much longer, it results in pressure drop value less than simulation 3 and almost the same as simulation 1 due to the reduction in cross-sectional area occupied by the protector.

Considering the erodible wear volume for geometry 1 and 4, the EWV is higher for geometry 4 and the protector in simulation 4 was therefore chosen as the best one that provides more EWV than geometry 1 with almost the same pressure drop.

Simulation	DP	EWV
Simulation 1	544	51.52
Simulation 2	499	51.52
Simulation 3	584	62.56
Simulation4	543	59.48

Table 6 Pressure drop and erodible wear volume

7.3 Post processing simulation results

The following figures show the velocity profile and pressure profile for the front part of the protector in direction of the flow (in X direction). The velocity profile, figure 35, shows that the maximum velocity value is at the clearance between the outer diameter of the protector and the tubing while the lowest value is in the front where there is a stagnation point, and behind the rib.
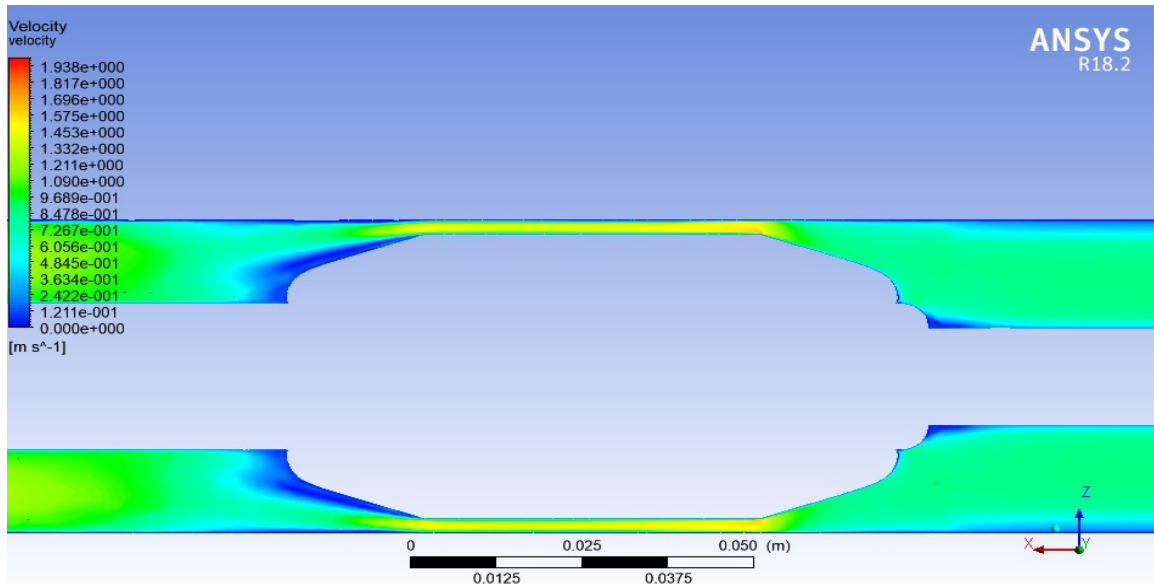

Figure 35 Velocity profile shows the front part of the protector

For the pressure profile, the highest value of pressure is at the leading surface which indicates the importance of the leading surface in pressure drop reduction. Reducing the angle of leading surface between the wear surface and the cylindrical body might help to reduce the pressure drop .
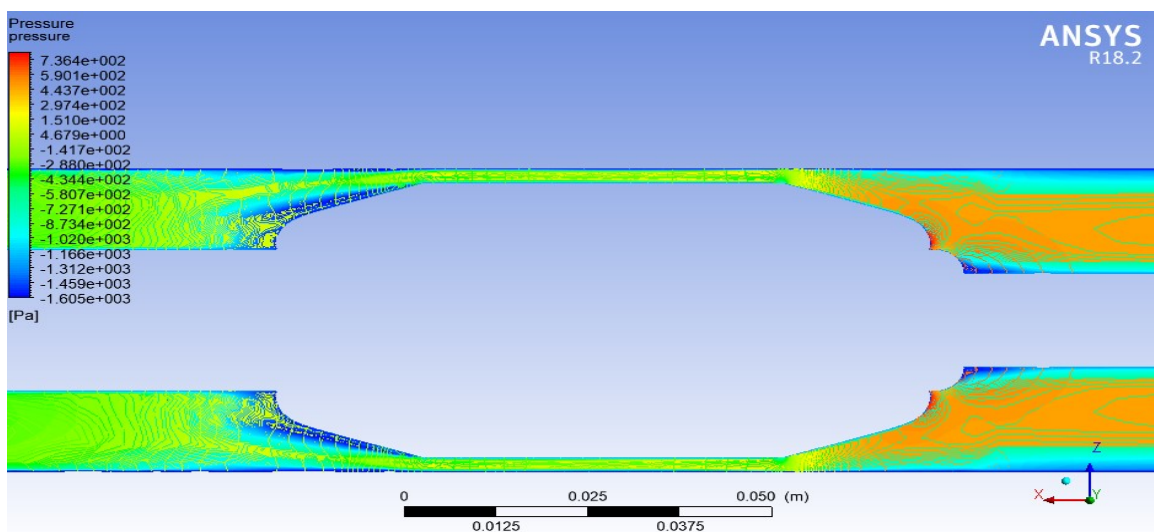

Figure 36 Pressure profile of the front part of the protector

8 Conclusion

The factors affecting the drag coefficient and the pressure drop of a protector are the cross-sectional area occupied by the protector with a selected inside tubing diameter and the length of the protector. The less the cross-sectional area, the less the pressure drop and drag coefficient. However, this reduction will affect the erodible wear volume as well which means there is a contradiction between the erodible wear volume and cross-sectional area.

Since increasing the length of the protector has less effects in increasing the drag coefficient and the pressure drop than decreasing the cross-sectional area, the protector can be made in longer length in order to compensate the loss of erodible wear volume due to the reduction of the cross-sectional area.

Producing a protector with smooth and streamlined surfaces especially in the leading surfaces of the ribs will further reduce the drag coefficient.

For the current design, a cross-sectional area less than 50 and L/D from 3.5 to 4 can provide the best results in terms of drag coefficient, pressure drop and erodible wear volume.

The calculations in chapter 5 shows that the holding grip, either the grip of the two part to each other or the protector to the cable, is a function of elasticity, friction and interference.

The advantages of the current design are therefore stated below:

- The protector is made of two identical parts, which can reduce the cost of producing the protector as a whole, and it can be easily installed on the wire rope at the well with holding grip depending on the material properties of the protector.
- The protector's design did follow the concepts above and as a result, it produced less pressure drop and drag coefficient than the patented rod guide mentioned before.
- The protector is suitable for the sucker rod pumps using wire ropes where the rod rotator can not be used to provide uniform erosion of the protector, because it provides scrapping effects of almost 360°.

9   Recommendations

In the following, some of the issues that need to be further investigated in order to improve the protector's functionality are described.

9.1 Materials

Protector materials as described in the chapter 4 should have certain mechanical, thermal and tribological properties like wear resistance and chemical resistance to all chemicals that might be used or encountered in wellbore. All those properties are responsible to extend the lifetime of the protector. The material has to meet also the requirements of NORSOK Standard M-710. New protector material is a significant project which can be conducted in Möntanuniversität Leoben as a cooperation between Department of Petroleum Engineering, Department of Polymer Engineering and Science, and Department of Metallurgy

9.2 Holding grip

Since the holding grip of the protector onto the cable is a concern, structural analysis (can be done using ANSYS or similar Software) should be carried out in order to analyse the forces that need to be maintained to hold the two parts of the protector together on the cable.

9.3 Design optimization

The next important stage is producing the protector and performing experiments for the pressure drop and the holding grip. This will provide real data to check the current results presented in this study, and also will help to optimize the design by providing validated data for the CFD simulation and structural analysis.

10 References

1. Lake, Larry W. Petroleum Engineering Handbook. 2007 : s.n.

2. Gabor Takacs, PhD. Sucker-Rod Pumping Handbook Production Engineering Fundamentals and Long-Stroke Rod Pumping. 2015.

3. National Oilwell Varco-Production Services. www.nov.com/tuboscope/. [Online] 2015. [Cited: Nov 1, 2018.] https://www.nov.com/WorkArea/DownloadAsset.aspx?id=16851.

4. Jun Xu, Ken Nolen, Dennis Shipp, Andy Cordova, Sam Gibbs Lufkin Automation. Rod Pumping Deviated Wells.

5. ROD GUIDE THEORY, SPACING METHODOLOGY, AND FIELD APPLICATION . W.L., Shellenberger F.A. and Foley. 1998, Southwestern Petroleum Short Course.

6. rod-guides. [Online] [Cited: 1 Jan 2018.] https://rfgpetrosystems.com/rod-guides/.

7. New High-Performance Field-Installed Sucker Rod Guides. T.P. Murtha, Phillips 66 Co., J. Pirtle, J.M. Huber Corp. and and W.B. Beaulieu, J.R. Waldrop,. 1987, Society of Petroleum Engineers .

8. Alberta Oil Tool, Product Line Overview. www.albertaoiltool.com. [Online] 2018. [Cited: Dec 15, 2018.] https://www.apergyals.com/assets/pdfs/AOT-PO.pdf.

9. National Oilwell Varco/Tuboscope /production Services. www.nov.com/tuboscope/. [Online] 2015. [Cited: 10 Nov 2018.] https://www.nov.com/WorkArea/DownloadAsset.aspx?id=16851.

10. Sucker r od Guide S - Shawcor. www.shawcor.com. [Online] [Cited: Dec 10, 2018.] https://cdn.shawcor.com/hg/medialibraries/shawcor/corporate/pdfs/sc_sucker_rod_gu ides_trifold-090817-2-page.pdf.

11. Abdo, Gary E. HELICAL ROD GUIDE AND METHOD. US 2007/0102151 A1 OK (US), 9 Nov 2005.

12. HELICAL SCRAPER APPARATUS FOR A RECIPROCATING SUCKER ROD. US 6,182,754 B1 1 Sep 1998.

13. Kaltwasser, Daryl. ROD GUIDE WITH WRAPPINGVANES. US 2012/0292021 A1 TX (US), 19 May 2011.

14. production-optimization/sucker-rod-guides. www.weatherford.com. [Online] 2018. [Cited: Dec 17, 2018.] https://www.weatherford.com/en/documents/brochure/products-and-services/production-optimization/sucker-rod-guides/.

15. Mabry, John F. SUCKER ROD GUIDE AND PARAFFIN SCRAPER FOR OIL WELLS. US 6,808,019 B1 6 Sep 2002.

16. —. SUCKER ROD GUIDE. US 9.200.489 B1 12 Aug 2013.

17. —. ROD GUIDE/PARAFFIN SCRAPER. 4,995,459 US, Jun 16, 1988.

18. Daryl Kaltwasser. PROGRESSIVE CAVITY PUMPROD GUIDE. US 2012/0168149 A1 TX (US), 4 Jan 2011.

19. www.global.weir/industries/oil-and-gas/ebrochure/. www.global.weir. [Online] 2014. [Cited: Dec 1, 2018.] https://www.global.weir/industries/oil-and-gas/ebrochure/seaboard-sucker-rod-guides.pdf.

20. WELL ROD, CENTRALIZER AND CENTRALIZER STOPINTERFACES WITH WEAR REDUCING SURFACE. 5,692,562 US, Sep 14, 1995.

21. Bair, Michael L. ROD COUPLING WITH MOUNTED GUIDE. 4,668,117 US, April 1, 1986.

22. products/wheeled-rod-guide. www.rodguides.com. [Online] [Cited: Dec 17, 2018.] http://rodguides.com/product/wheeled-rod-guide.

23. the best plastic materials for high friction applications. www.craftechind.com. [Online] [Cited: Oct 5, 2018.] http://www.craftechind.com/the-best-plastic-materials-for-high-friction-applications/.

24. Bell, Dr. Joel. Wear Resistant Thermoplastic compounds. www.rtpcompany.com. [Online] [Cited: Nov 8, 2018.] https://www.rtpcompany.com/products/wear-resistant/.

25. Amodel® PPA Design Guide. www.solvay.com. [Online] 2014. [Cited: Dec 24, 2018.] https://www.solvay.com/sites/g/files/srpend221/files/2018-08/Amodel-PPA-Design-Guide_EN-5.0_0.pdf.

26. Biron, Michel. Material Selection for Thermoplastic Parts . s.l. : Elsevier Ltd, 2016.

27. Rod Guides. petrowiki.org. [Online] March 8, 2018. [Cited: Nov 2, 2018.] https://petrowiki.org/Rod_guides.

28. Olinger, Edward L. LOW TURBULENCE ROD GUIDE. 5,115,863 US, April 5, 1991.

29. Tehrani, Fatemeh Fazeli. Analysis and Simulation of a High-Performance Wire and Fibre Rope as Continuous Sucker Rod String. Montan University : s.n., 2016.

30. Dieter Muhs, Herbert Wittel,Dieter Jannasch,Joachim Voßiek. Roloff / Matek Maschinenelemente. Wiesbaden : Friedr. Vieweg & Sohn Verlag , 2007.

31. Bonenberger, Paul R. The First Snap-Fit Handbook. Munich : Carl Hanser Verlag, 2016.

32. Snap-Fit Joints for Plastics - A Design Guide. [Online] http://fab.cba.mit.edu/classes/S62.12/people/vernelle.noel/Plastic_Snap_fit_design.pdf ..

33. ANSYS Fluent User's Guide. s.l. : ANSYS, Inc, 2013.

34. Hall, Nancy. the drag coefficient. NASA. [Online] May 5, 2015. https://www.grc.nasa.gov/WWW/K-12/airplane/dragco.html.

35. Sable, Donald E. ROD GUIDE. 4575163 U.S. C, 31 Dec 1984.

36. Davison, Matthew S. ROD GUIDE WITH IMPROVED STATOR. US 2009/0183885 A1 OK (US, 23 Jan 2008.

37. WELL ROD, CENTRALIZER AND CENTRALIZER STOPINTERFACES WITH. 5,692,562 US, 14 Sep 1995.

38. Hart, Charles M. FIELD INSTALLED SLOTTED ROD GUIDE AND METHOD. 5,549,158 US, May 9, 1995.

39. Sable, Donald E. ROD GUIDE ASSEMBLY AND METHOD OF TSNSTALLATION ON A ROD SHANK. 5,191,938 US, Dec 16 1991.

40. Qualification of non-metallic sealing materials and manufactures. NORSOK STANDARD M-710. October 2, 2011.

41. norrisglobal/products/rod-guides/standard-rod-guides. http://www.npsportal.com. [Online] 2015. [Cited: Nov 3, 2018.] http://www.npsportal.com/norrisrods/en/norrisglobal/products/rod-guides/standard-rod-guides.

42. Abdelbary, Ahmed. Wear of Polymers and Composites . s.l. : Woodhead Publishing, UK., 2014.

43. rod guide materials for all levels of performance - RTP Company. http://www.rtpcompany.com. [Online] 2014. [Cited: Nov 26, 2018.] http://www.rtpcompany.com/wp-content/uploads/2014/05/Rod_Guide.pdf.

44. Guide for the Verification and Validation of Computational Fluid Dynamics Simulations. 1998, American Institute of Aeronautics and Astronautics.

List of Tables

Table of equations

Table of figures

Nomenclature

OD   Outside tubing diameter [mm]

ID   Inside tubing diameter [mm]

Fmax   Maximum compressive force radius [N]

Fax   Axial force [N]

Fn   Normal force [N]

Sr   Safety factor

μ   Coefficient of friction

y   Permissible deflection [mm]

ρ Density [kg/m^3].

b   length of the beam [mm]

h   Thickness of the beam [mm]

w   Width of the beam [mm]

Es   Secant Modulus [Mpa]

I   Turbulence intensity

Rh   Reynolds number

D   Hydraulic diameter [mm]

V   Fluid velocity [m/s]

Cd   Drag coefficient

Df   Drag force [N]

A   Surface area [mm]

Θ   Angle of attack [degree]

f Friction factor

l/D   Length to diameter of the protector

Appendices

Appendix A - Material Datasheet

CAMPUS® Datasheet

VESTAKEEP® L 4000 G - PEEK
Evonik Industries AG

EVONIK
POWER TO CREATE

Product Texts

VESTAKEEP® L 4000 G

VESTAKEEP® L 4000 G is a high viscosity, unreinforced polyether ether
ketone for injection molding and extrusion.
The semi-crystalline polymer features superior thermal and chemical resistance.
Parts made from **VESTAKEEP® L 4000 G** are self-extinguishing.

VESTAKEEP® L 4000 G can be processed on common machines for
thermoplastics.

Application example: Parts for the electrical industry,
machinery construction and aerospace.

Rheological properties	Value	Unit	Test Standard
Melt volume-flow rate, MVR	12	cm³/10min	ISO 1133
Temperature	380	°C	ISO 1133
Load	5	kg	ISO 1133
Molding shrinkage, parallel	1.1	%	ISO 294-4, 2577
Molding shrinkage, normal	1.8	%	ISO 294-4, 2577

Mechanical properties	Value	Unit	Test Standard
Tensile modulus	3500	MPa	ISO 527-1/-2
Yield stress	96	MPa	ISO 527-1/-2
Yield strain	5	%	ISO 527-1/-2
Nominal strain at break	30	%	ISO 527-1/-2
Charpy impact strength, +23°C	N	kJ/m²	ISO 179/1eU
Charpy impact strength, -30°C	N	kJ/m²	ISO 179/1eU
Charpy notched impact strength, +23°C	7	kJ/m²	ISO 179/1eA
Charpy notched impact strength, -30°C	6	kJ/m²	ISO 179/1eA

Thermal properties	Value	Unit	Test Standard
Melting temperature, 10°C/min	340	°C	ISO 11357-1/-3
Temp. of deflection under load, 1.80 MPa	155	°C	ISO 75-1/-2
Temp. of deflection under load, 0.45 MPa	205	°C	ISO 75-1/-2
Vicat softening temperature, 50°C/h 50N	305	°C	ISO 306
Coeff. of linear therm. expansion, parallel	60	E-6/K	ISO 11359-1/-2
Burning Behav. at 1.5 mm nom. thickn.	V-0	class	IEC 60695-11-10
Thickness tested (1.5)	1.6	mm	IEC 60695-11-10
Oxygen index	38	%	ISO 4589-1/-2

Electrical properties	Value	Unit	Test Standard
Relative permittivity, 100Hz	2.8	-	IEC 62631-2-1
Relative permittivity, 1MHz	2.8	-	IEC 62631-2-1
Dissipation factor, 1MHz	50	E-4	IEC 62631-2-1
Volume resistivity	>1E13	Ohm*m	IEC 62631-3-1
Surface resistivity	1E15	Ohm	IEC 62631-3-2
Comparative tracking index	200	-	IEC 60112

VESTAKEEP® L 4000 G - PEEK
Evonik Industries AG

Other properties	Value	Unit	Test Standard
Water absorption	**0.5**	%	Sim. to ISO 62
Density	**1300**	kg/m³	ISO 1183

Rheological calculation properties	Value	Unit	Test Standard
Thermal conductivity of melt	**0.18**	W/(m K)	-
Spec. heat capacity melt	**2110**	J/(kg K)	-

Test specimen production	Value	Unit	Test Standard
Injection Molding, melt temperature	**370**	°C	ISO 294
Injection Molding, mold temperature	**180**	°C	ISO 294
Injection Molding, injection velocity	**200**	mm/s	ISO 294
Injection Molding, pressure at hold	**120**	MPa	ISO 294

Diagrams

Stress-strain

Secant modulus-strain

Stress-strain
VESTAKEEP® L 4000 G
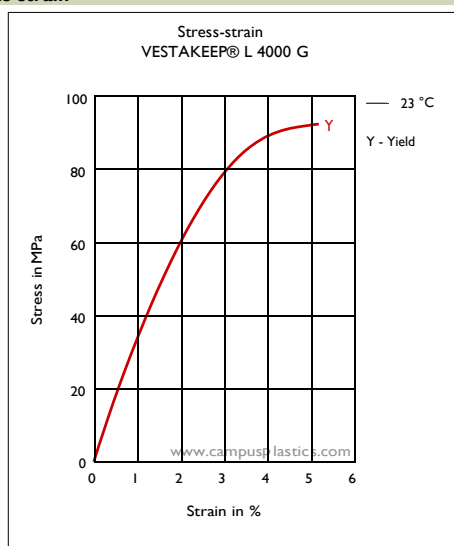
Secant modulus-strain
VESTAKEEP® L 4000 G
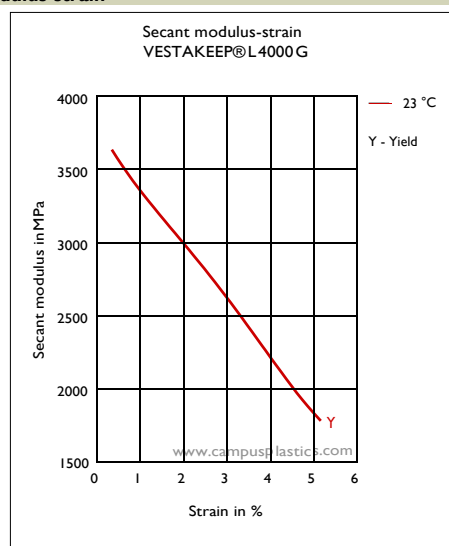
Characteristics

Processing
Injection Molding, Film Extrusion, Other Extrusion

Delivery form
Pellets

Regional Availability
North America, Europe, Asia Pacific, South and Central America, Near East/Africa

Appendix B – Drawing of geometry 1

Ø 23.70

85°

16.01

A (1 : 1)

148.00

140.00

68.68

28.89

R4.00